pressurized with a further 3 mL perfluoropropane gas. The vial was placed in a bath-type sonicator (42 kHz, 100 W) (BRANSONIC 2510j-DTH; Branson Ultrasonics Co.) for 5 min to form BLs.

Flow cytometry analysis

To evaluate the cellular association of liposomes, the day before experiments, KB cells (1×10^5) were seeded in a 12-well plate. 0.2 mol% DiI-labeled folate-PEG liposomes (pDNA: 3 μg/mL) were added to the cells and incubated for 1 h at 37°C. To examine the cellular uptake pathway of folate-PEG liposomes, the cells were incubated with chlorpromazine (10 μg/mL), genistein (400 μM) or amiloride (1 mM) for 30 min and then treated with DiI-labeled folate-PEG liposomes in the presence of endocytic inhibitor for a further 1 h at 37°C. The cells were then collected and the fluorescence intensities were measured by flow cytometry (BD FACSCanto, Franklin Lakes, NJ). The mean fluorescence intensity of cells was quantified. The results are presented as a mean ± SD obtained from three sample ($n = 3$).

Confocal laser scanning microscopy

KB cells were seeded the day before the experiments. 0.2 mol% DiI-labeled folate-PEG liposomes (pDNA: 3 μg/mL) were added to the cells and incubated for 1 h at 37°C. After incubation, the cells were fixed with 4% paraformaldehyde for 1 h at 4°C, followed by CLSM (FV1000D; Olympus Corporation, Tokyo, Japan).

Transfection of pDNA into cells using folate-PEG liposomes

The day before the experiments, KB cells (3×10^4) were seeded in a 48-well plate. The cells were treated with folate-PEG liposomes (encapsulated pDNA: 3 μg/mL) in serum-free medium for 4 h at 37°C. The cells was also treated with pDNA and Lipofectamine$_{2000}$ (Invitrogen Japan K.K., Tokyo, Japan) complexes prepared according to the manufacturer's instructions for 4 h. After replacement with fresh medium, the cells were cultured for 20 h and then luciferase activity was measured.

Transfection of pDNA into cells by combination of folate-PEG liposomes with BLs and US exposure

The day before the experiments, KB cells (3×10^4) were seeded in a 48-well plate. The cells were treated with folate-PEG liposomes (encapsulated pDNA: 3 μg/mL) in serum-free medium for 4 h at 37°C. After incubation, the cells were washed twice within 10 min to remove any excess folate-PEG liposomes that were not associated with the cells and BLs (60 μg/well) were added. Within 2 min, US exposure was applied through a 6 mm diameter probe placed in the well (frequency, 2 MHz; duty, 50%; burst rate, 2 Hz; intensity, 1.0 W/cm^2; time, 10 s). A Sonopore 3000 (NEPA GENE, Co., Ltd., Chiba, Japan) was used to generate the US exposure. The cells were cultured for 20 h, and then luciferase activity was determined and cell viability was measured using a WST-8 assay (Cell Counting Kit-8; Dojindo Laboratories, Kumamoto, Japan).

Measurement of luciferase expression

Cell lysate was prepared with lysis buffer (0.1 M Tris-HCl (pH 7.8), 0.1% Triton X-100, and 2 mM EDTA). Luciferase activity was measured using a luciferase assay system (Promega, Madison, WI) and a luminometer (LB96 V; Belthold Japan Co. Ltd., Tokyo, Japan). Activity is indicated as relative light units (RLU) per mg protein ± SD, four independent determinations were performed for each transfection experiment ($n = 4$).

Statistical analysis

Statistical analyses were performed to establish the significance of variation using Student's t-test. Differences with a value of $p < 0.05$ were considered statistically different.

Results

Physical properties of prepared liposomes

We prepared non-labeled PEG liposomes and folate-PEG liposomes encapsulating pDNA condensed by protamine as a model to evaluate the utility of BLs and US exposure in general. We first examined the physical properties of prepared liposomes. The average size and zeta potential of prepared liposomes were about 150 nm and with a positive charge (Table 1).

Cellular association and internalization of folate-PEG liposomes

We evaluated the effect of folate labeling on the cellular association and internalization of liposomes. KB cells were incubated with either non-labeled PEG liposomes or folate-PEG liposomes containing DiI for 1 h at 37°C, and fluorescence intensity was examined by flow cytometry. The cells treated with folate-PEG liposomes showed enhanced fluorescence intensity compared with non-labeled PEG liposomes (Figure 1a). The mean fluorescence intensity of cells treated with folate-PEG liposomes was significantly increased compared with that of cells treated with non-labeled PEG liposomes ($p < 0.05$) (Figure 1b). To elucidate the subcellular localization of liposomes after uptake by folate receptor, folate-PEG liposomes containing DiI were monitored in the cells by confocal laser scanning microscopy (CLSM). In cells treated with folate-PEG liposomes, the fluorescence of liposomes was observed in the cytoplasm after incubation for 1 h. In contrast, the fluorescence of liposomes was weak in the cytoplasm of cells treated with non-labeled

Table 1. Physical properties of prepared liposomes.

Prepared liposomes	PEG liposomes	Folate-PEG liposomes
Particle size(nm)	148.9 ± 20.7	146.6 ± 5.9
z potential (mV)	13.37 ± 0.6	18.46 ± 2.3

Data represent means and SD of three different determinations.

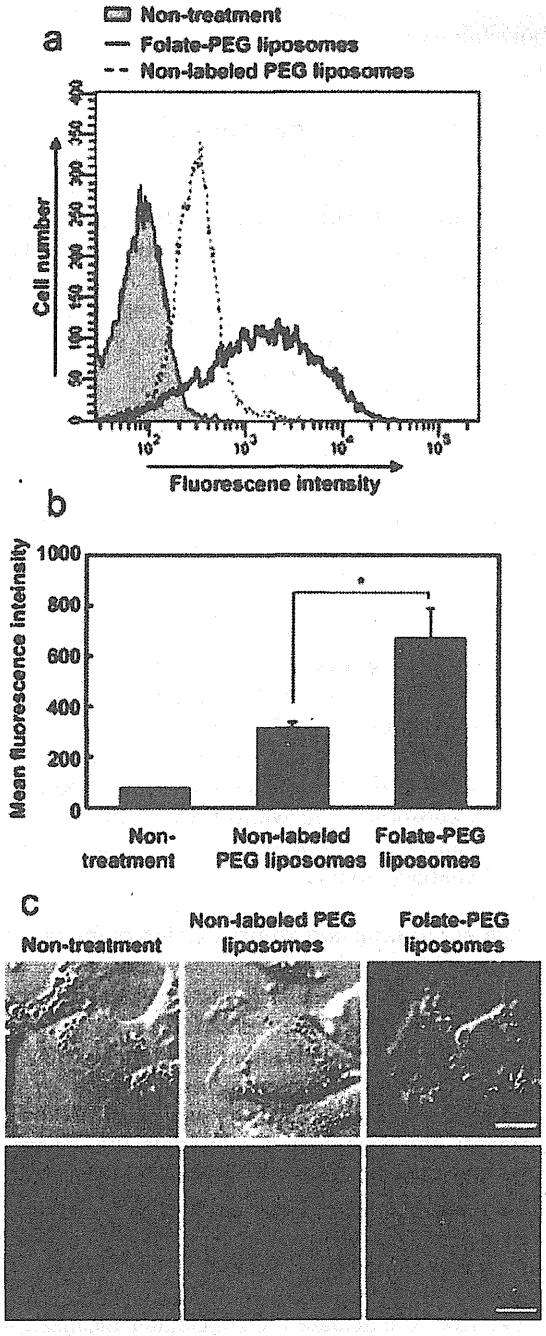

Figure 1. Cellular association and internalization of folate-PEG liposomes. KB cells were treated with DiI-labeled, non-labeled or folate-PEG liposomes for 1 h at 37°C. (a) Fluorescence intensity was measured by flow cytometry. (b) The mean fluorescence intensity of cells was quantified. (c) Cells were observed by CLSM. Scale bars represent 10 μm. Data are the means ± SD ($n = 3$). *$p < 0.05$.

PEG liposomes (Figure 1c). These results suggested that folate-PEG liposomes could efficiently associate with and internalize into cells.

Endocytic pathway of folate-PEG liposomes

It is possible that the difference in the cellular uptake pathway of carriers may affect the enhancement of transfection efficiency by BLs and US exposure. We assessed the endocytic pathway of folate-PEG liposomes using several inhibitors. We evaluated the involvement of clathrin-mediated endocytosis, raft-dependent endocytosis, and macropinocytosis in the cellular uptake of folate-PEG liposomes. To inhibit clathrin-mediated endocytosis, KB cells were treated with chlorpromazine, which blocks the assembly of coated pits at the plasma membrane (Wang et al., 1993). Raft-dependent endocytosis was inhibited by genistein, which is a thyrosin kinase inhibitor (Pelkmans et al., 2002). We also used amiloride, a specific inhibitor of the Na^+/H^+ exchange required for macropinocytosis (Wadia et al., 2004). The cells were treated with DiI-labeled folate-PEG liposomes in the presence or absence of several inhibitors, and fluorescence intensity of cells was measured by flow cytometry. As shown in Figure 2, when the cells were treated with genistein, fluorescence intensity was significantly decreased compared with that of folate-PEG liposomes in the absence of genistein. The fluorescence intensity of folate-PEG liposomes was slightly decreased by treatment of chlorpromazine and amirolide. The mean fluorescence intensity of cells treated with genistein or chlorpromazine was decreased compared with that of folate-PEG liposomes in the absence of endocytic inhibitors ($p < 0.05$) (Figure 2b). These results suggested that raft-dependent endocytosis was the major cellular uptake pathway of folate-PEG liposomes, and they could partially internalize into cells via clathrin-mediated endocytosis and macropinocytosis.

Endosomal escape of folate-PEG liposomes

Folate-PEG liposomes were efficiently associated with cells and internalized into cells via raft-dependent endocytosis, whereas it is needed to deliver genes to cytosol efficiently from endosomes to obtain high gene expression. We next examined the efficacy of endosomal escape in folate-PEG liposomes. KB cells were treated with non-labeled or folate-PEG liposomes in the presence or absence of chloroquine, which is considered an endosomolytic agent (Sonawane et al., 2003). KB cells were transfected by non-labeled or folate-PEG liposomes with or without chloroquine. The resulting luciferase activity of folate-PEG liposomes with chloroquine was sevenfold higher than that of folate-PEG liposomes without chloroquine ($p < 0.05$) (Figure 3). It was suggested that folate-PEG liposomes could not deliver genes into cytosol from endosomes sufficiently, although they could internalize into cells.

Enhanced gene transfection of folate-PEG liposomes by BLs and US exposure

Our previous study showed that BLs and US exposure could improve endosomal escape, leading to enhancement of the gene transfection efficiency of AG73-PEG liposomes. Folate-PEG liposomes could not deliver genes into cytosol from endosomes sufficiently and there was

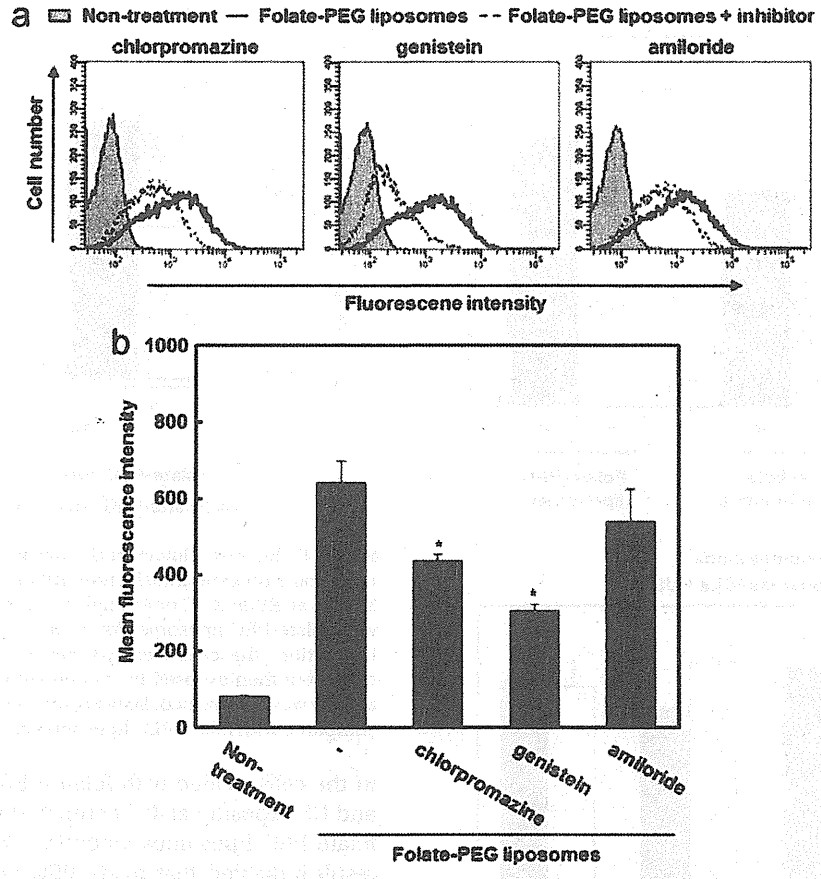

Figure 2. Endocytic pathway of folate-PEG liposomes. KB cells were incubated with chlorpromazine (10 μg/mL), genistein (400 μM) or amiloride (1 mM) for 30 min and then treated with DiI-labeled folate-PEG liposomes in the presence of endocytic inhibitors for a further 1 h at 37°C. (a) Fluorescence intensity was measured by flow cytometry. (b) The mean fluorescence intensity of cells was quantified. Data are the means ± SD ($n = 3$). *$p < 0.05$ compared with folate-PEG liposomes without endocytic inhibitor.

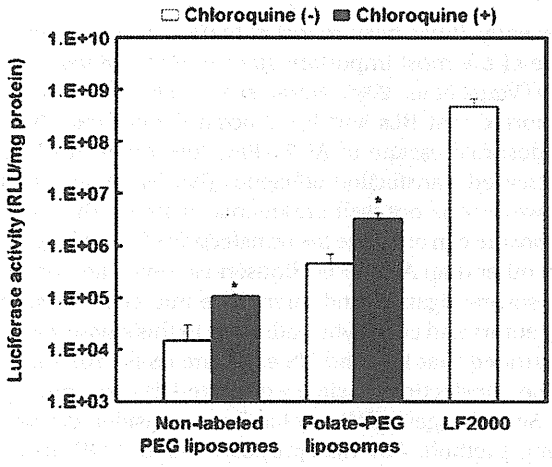

Figure 3. Endosomal escape of folate-PEG liposomes. KB cells were preincubated with chloroquine (200 μM) for 30 min before transfection and then treated with non-labeled or folate-PEG liposomes in the presence of chloroquine for a further 4 h at 37°C. The cells were also transfected by Lipofectamine$_{2000}$ (LF2000) for 4 h. After replacement with fresh medium, the cells were cultured for 20 h and then luciferase activity was determined. Data are the means ± SD ($n = 4$). *$p < 0.05$ compared with liposomes without chloroquine.

the potential to improve transfection efficiency by BLs and US exposure. To investigate the effect of BLs and US exposure on gene transfection of folate-PEG liposomes, KB cells were incubated with folate-PEG liposomes for 4 h at 37°C, and then the cells were treated with BLs and US exposure. As a result, luciferase activity was enhanced up to about five-fold by treatment with BLs and US exposure compared with folate-PEG liposomes alone. Furthermore, the luciferase activity of folate-PEG liposomes with BLs and US exposure was five-fold higher than that of non-labeled PEG liposomes with BLs and US exposure ($p < 0.05$) (Figure 4a). We also examined the cytotoxicity of the treatment of folate-PEG liposomes with BLs and US exposure. Significant cytotoxicity was not observed, and cell viability was more than 80% even after each transfection (Figure 4b). These results suggested that BLs and US exposure could enhance the transfection efficiency of folate-PEG liposomes without significant cytotoxicity.

Effect of folate-PEG liposomes attached to the cell membrane on gene transfection

It is reported that BLs and US exposure could increase the permeability of the cell membrane. It is possible that

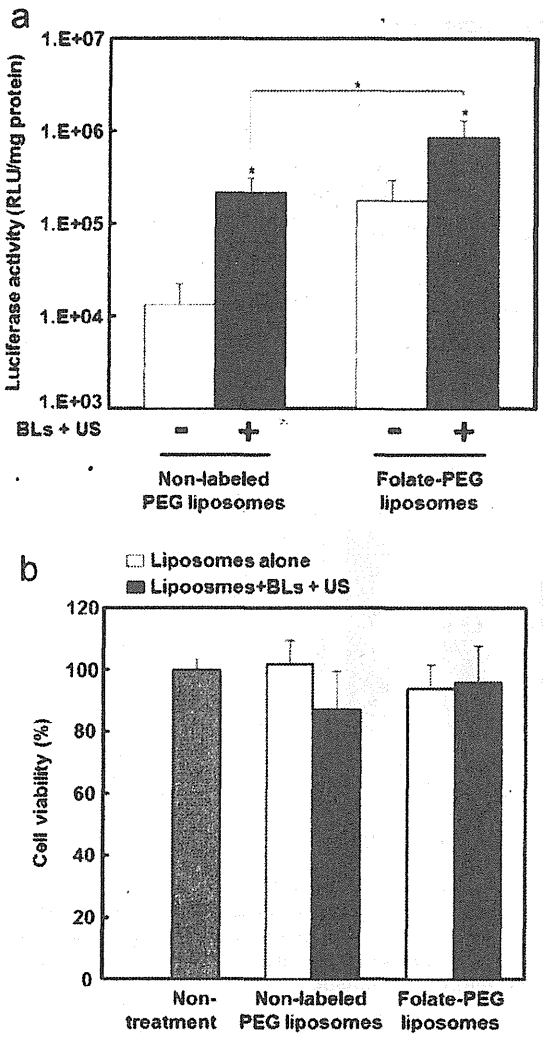

Figure 4. Enhanced gene transfection of folate-PEG liposomes by BLs and US exposure. KB cells were treated with non-labeled or folate-PEG liposomes for 4 h. The cells were washed and treated with BLs (60 μg) and US exposure. The cells were incubated for 20 h and then (a) luciferase activity was determined and (b) cell viability was measured using a WST-8 assay. Data are the means ± SD ($n = 4$). *$p < 0.05$ compared with folate-PEG liposomes alone.

BLs and US exposure enhance the direct internalization of folate-PEG liposomes. Therefore, we evaluated the involvement of folate-PEG liposomes attached to the surface of the cell membrane in enhanced gene transfection. KB cells were transfected with folate-PEG liposomes with or without BLs and US exposure at 37°C or 4°C, and the luciferase activity was measured. It is known that endocytosis is inhibited at 4°C. Therefore, folate-PEG liposomes cannot internalize into cells at 4°C. In contrast, Folate-PEG liposomes associate with cell membrane and internalize into cells at 37°C. When the cells were treated with folate-PEG liposomes with BLs and US exposure at 37°C, the luciferase activity was increased compared with that of the cells treated with folate-PEG liposomes alone ($p < 0.05$). In contrast, the luciferase activity did not change

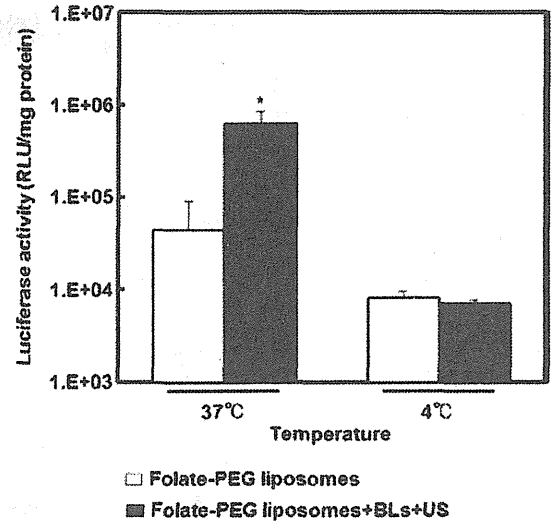

Figure 5. Effect of folate-PEG liposomes attached to the cell membrane on gene transfection. KB cells were preincubated for 30 min at either 37°C or 4°C before transfection and then treated with folate-PEG liposomes for a further 1 h at 37°C or 4°C. After incubation, the cells were washed and BLs were added. The cells were then exposed to US and cultured for 23 h. Luciferase activity was determined. Data are the means ± SD ($n = 4$). *$p < 0.05$ compared with folate-PEG liposomes alone.

in the cells treated with folate-PEG liposomes with BLs and US exposure at 4°C compared with the treatment of folate-PEG liposomes alone ($p > 0.05$) (Figure 5). This result indicated that folate-PEG liposomes attached to the cell membrane could not involve in the enhanced gene transfection by BLs and US exposure.

Discussion

Recently, it has been reported that endosomal escape is one of the most important steps in efficient gene delivery (Varga et al., 2005; Hama et al., 2006). We previously reported that BLs and US exposure could improve the endosomal escape of AG73-PEG liposomes, leading to increased transfection efficiency (Negishi et al., 2010b); however it is not well understood whether BLs and US exposure can enhance the transfection efficiency of carriers other than AG73-PEG liposomes, which are modified by several ligands, and internalize into cells via several receptors and endocytic pathways. In this study, we demonstrated that BLs and US exposure could enhance the gene transfection efficiency of folate-PEG liposomes.

Selective gene delivery has been considered a promising method. For this purpose, folate, RGD peptide, transferrin, and anisamide have been used as ligands to develop selective gene delivery carriers (Li et al., 2008; Ng et al., 2009; Koppu et al., 2010; Morris & Sharma 2011). Folate receptor is expected to be a specific receptor of cancer cells, and folate-modified carriers have been developed to achieve selective gene delivery. The majority of these carriers were internalized via endocytosis and required to deliver genes from endosomes to cytosol for

high gene expression. For efficient endosomal escape, some studies developed folate-modified carriers, which function to enhance endosomal escape (Shi et al., 2002); therefore, we chose folate-modified liposomes as a model to assess the utility of BLs and US exposure in general. In this study, to evaluate whether BLs and US exposure can be generally applied to gene delivery carriers to improve transfection efficiency, we examined whether BLs and US exposure can enhance the gene transfection efficiency of folate-PEG liposomes.

We previously reported that AG73-PEG liposomes were partially internalized into cells via clathrin-mediated endocytosis and syndecan, a heparan sulfate-containing transmembrane proteoglycan (Negishi et al., 2010b), whereas the cellular uptake pathway of folate-PEG liposomes was mainly raft-dependent endocytosis via folate receptor (Figures 1, 2). Our result also showed that BLs and US exposure could enhance the transfection efficiency of folate-PEG liposomes (Figure 4a). These results suggested that BLs and US exposure could enhance the transfection efficiency of carriers, which were internalized via various receptors and endocytic pathways in different cell lines; however, we could not assess the effect of BLs and US exposure on carriers, which internalized into cells via macropinocytosis. Further study is required of the involvement of the uptake pathway in enhanced gene transfection by BLs and US exposure.

On the other hand, it is reported that high transfection activity is required to overcome rate-limiting steps such as cellular internalization, endosomal escape, and nuclear transfer (Varga et al., 2005; Hama et al., 2006). PEG modification has the advantage of increasing the stability of carriers *in vivo*, but it is also believed to suppress cellular association and/or endosomal escape of carriers and to decrease gene expression (Zalipsky et al., 1999; Guo & Szoka, 2001; Shin et al., 2003; Walker et al., 2005; Hatakeyama et al., 2007). Indeed, the present study also showed that folate-PEG liposomes could not deliver genes into cytosol from endosomes sufficiently (Figure 3); therefore, endosomal escape is an important step to achieve efficient gene delivery. Our previous study demonstrated that BLs and US exposure could enhance the endosomal escape of AG73-PEG liposomes (Negishi et al., 2010b). In contrast, we and other groups reported that microbubbles and US exposure increased the permeability of the cell membrane, and delivered genes into the cytoplasm directly (Taniyama et al., 2002; Lentacker et al., 2009; Negishi et al., 2008; Suzuki et al., 2010; Negishi et al., 2011). Hence, we assessed the involvement of folate-PEG liposomes attached to the surface of cell membrane in enhanced gene transfection. Our results indicated that enhanced gene transfection by BLs and US exposure did not rely on folate-PEG liposomes associating with cell membrane (Figure 5). It was suggested that BLs and US exposure could affect intracellular trafficking of folate-PEG liposomes, leading to increased gene expression in the same manner as AG73-PEG liposomes.

When we compared Figure 3 and Figure 4, the transfection efficiency of folate-PEG liposomes with chloroquine was higher than that of the treatment with BLs and US exposure. It is possible that BLs and US exposure in further optimized condition may increase the transfection efficiency of folate-PEG liposomes up to that of chloroquine treatment. On the other hand, we need to concern that chloroquine cannot target some tissue and cells *in vivo*. In contrast, BLs and US exposure have advantage that the effect may be induced in the specific area focused US. Therefore, it is expected that BLs and US may enhance the transfection efficiency of gene delivery carriers in targeted tissues and cells.

However, we should investigate the more specific mechanism by which BLs and US exposure may affect directly intracellular vesicle morphology or induce several biological effects. It has been reported that microbubbles and US exposure induced the influx of calcium ions (Juffermans et al., 2008; Zhou et al., 2008; Kumon et al., 2009), and acidification of endosomes was regulated by calcium ions (Lelouvier et al., 2011); therefore, we will elucidate in a further study whether BLs and US exposure induce the influx of calcium ions and destabilize endosomes. We may also need to examine more clearly the effect of BLs and US exposure on transcription and other organelles. There is a possibility that several biological effects concerning gene transfection are induced by BLs and US exposure, and can affect, at least, folate-PEG liposomes internalized into cells (Figure 5) and improve intracellular trafficking of folate-PEG liposomes in the same manner as AG73-PEG liposomes.

We have reported that BLs and US exposure could enhance the transfection efficiency of AG73-PEG liposomes by about sixty-fold compared with AG73-PEG liposomes alone. On the other hand, the transfection efficiency of folate-PEG liposomes was enhanced up to five-fold by BLs and US exposure. These results suggested that BLs and US exposure had more influence on the transfection efficiency of AG73-PEG liposomes. The difference in the extent of enhanced transfection efficiency might be dependent on the different endocytic pathways and receptors that carriers mediate. The sensitivity of BLs and US exposure to different cell lines might also influence the efficacy of endosomal escape, leading to increased gene transfection; therefore, it is important, in order to achieve efficient gene transfection, that we understand the factors influencing the efficacy of endosomal escape. Although more study is required of the detailed mechanism of enhanced gene transfection, we expect that BLs and US exposure will be a promising method to achieve efficient endosomal escape, and this method may be applied in existing carriers, and peptide or protein delivery, which suffers from low endosomal escape.

Conclusions

We previously reported that BLs and US exposure could enhance endosomal escape and gene transfection of

AG73-PEG liposomes, which were internalized into cells via syndecan and partially clathrin-mediated endocytosis (Negishi et al., 2010b). In this study, we evaluated whether BLs and US exposure could be applied to other carriers, and assessed the utility of BLs and US exposure in general. The present study showed the enhanced transfection efficiency of folate-PEG liposomes, which are internalized into cells via folate receptor and raft-dependent endocytosis, when BLs and US exposure was applied. Our results suggested that BLs and US exposure could enhance endosomal escape and transfection efficiency of folate-PEG liposomes in the same manner as for AG73-PEG liposomes; thus, BLs and US exposure may be a promising method in general to achieve efficient gene transfection using various gene carriers.

Acknowledgments

We are grateful to Katsuro Tachibana (Department of Anatomy, School of Medicine, Fukuoka University) for technical advice regarding the induction of cavitation with US, and to Yasuhiko Hayakawa and Kosho Suzuki (NEPA GENE Co., Ltd) for technical advice regarding exposure to US.

Declaration of interest

This study was supported by an Industrial Technology Research Grant (04A05010) from the New Energy and Industrial Technology Development Organization (NEDO) of Japan, a Grant-in-aid for Exploratory Research (18650146) and a Grant-in-aid for Scientific Research (B) (20300179) from the Japan Society for the Promotion of Science, and by a grant for private universities provided by the Promotion and Mutual Aid Corporation for Private Schools of Japan.

The authors report no declaration of interest.

References

Dewey RA, Morrissey G, Cowsill CM, Stone D, Bolognani F, Dodd NJ, Southgate TD, Klatzmann D, Lassmann H, Castro MG, Löwenstein PR. (1999). Chronic brain inflammation and persistent herpes simplex virus 1 thymidine kinase expression in survivors of syngeneic glioma treated by adenovirus-mediated gene therapy: implications for clinical trials. Nat Med, 5, 1256–1263.

Garin-Chesa P, Campbell I, Saigo PE, Lewis JL Jr, Old LJ, Rettig WJ. (1993). Trophoblast and ovarian cancer antigen LK26. Sensitivity and specificity in immunopathology and molecular identification as a folate-binding protein. Am J Pathol, 142, 557–567.

Guo X, Szoka FC Jr. (2001). Steric stabilization of fusogenic liposomes by a low-pH sensitive PEG-diortho ester-lipid conjugate. Bioconjug Chem, 12, 291–300.

Hama S, Akita H, Ito R, Mizuguchi H, Hayakawa T, Harashima H. (2006). Quantitative comparison of intracellular trafficking and nuclear transcription between adenoviral and lipoplex systems. Mol Ther, 13, 786–794.

Hatakeyama H, Akita H, Kogure K, Oishi M, Nagasaki Y, Kihira Y, Ueno M, Kobayashi H, Kikuchi H, Harashima H. (2007). Development of a novel systemic gene delivery system for cancer therapy with a tumor-specific cleavable PEG-lipid. Gene Ther, 14, 68–77.

Hatakeyama H, Ito E, Akita H, Oishi M, Nagasaki Y, Futaki S, Harashima H. (2009). A pH-sensitive fusogenic peptide facilitates endosomal escape and greatly enhances the gene silencing of siRNA-containing nanoparticles *in vitro* and *in vivo*. J Control Release, 139, 127–132.

Hirko A, Tang F, Hughes JA. (2003). Cationic lipid vectors for plasmid DNA delivery. Curr Med Chem, 10, 1185–1193.

Høgset A, Prasmickaite L, Selbo PK, Hellum M, Engesaeter BØ, Bonsted A, Berg K. (2004). Photochemical internalisation in drug and gene delivery. Adv Drug Deliv Rev, 56, 95–115.

Juffermans LJ, Kamp O, Dijkmans PA, Visser CA, Musters RJ. (2008). Low-intensity ultrasound-exposed microbubbles provoke local hyperpolarization of the cell membrane via activation of BK(Ca) channels. Ultrasound Med Biol, 34, 502–508.

Kawano K, Onose E, Hattori Y, Maitani Y. (2009). Higher liposomal membrane fluidity enhances the *in vitro* antitumor activity of folate-targeted liposomal mitoxantrone. Mol Pharm, 6, 98–104.

Kibria G, Hatakeyama H, Ohga N, Hida K, Harashima H. (2011). Dual-ligand modification of PEGylated liposomes shows better cell selectivity and efficient gene delivery. J Control Release, 153, 141–148.

Koppu S, Oh YJ, Edrada-Ebel R, Blatchford DR, Tetley L, Tate RJ, Dufès C. (2010). Tumor regression after systemic administration of a novel tumor-targeted gene delivery system carrying a therapeutic plasmid DNA. J Control Release, 143, 215–221.

Kumon RE, Aehle M, Sabens D, Parikh P, Han YW, Kourennyi D, Deng CX. (2009). Spatiotemporal effects of sonoporation measured by real-time calcium imaging. Ultrasound Med Biol, 35, 494–506.

Leamon CP, Cooper SR, Hardee GE. (2003). Folate-liposome-mediated antisense oligodeoxynucleotide targeting to cancer cells: evaluation *in vitro* and *in vivo*. Bioconjug Chem, 14, 738–747.

Lee SH, Choi SH, Kim SH, Park TG. (2008). Thermally sensitive cationic polymer nanocapsules for specific cytosolic delivery and efficient gene silencing of siRNA: swelling induced physical disruption of endosome by cold shock. J Control Release, 125, 25–32.

Lelouvier B, Puertollano R. (2011). Mucolipin-3 regulates luminal calcium, acidification, and membrane fusion in the endosomal pathway. J Biol Chem, 286, 9826–9832.

Lentacker I, Wang N, Vandenbroucke RE, Demeester J, De Smedt SC, Sanders NN. (2009). Ultrasound exposure of lipoplex loaded microbubbles facilitates direct cytoplasmic entry of the lipoplexes. Mol Pharm, 6, 457–467.

Li SD, Chono S, Huang L. (2008). Efficient oncogene silencing and metastasis inhibition via systemic delivery of siRNA. Mol Ther, 16, 942–946.

Mäe M, El Andaloussi S, Lundin P, Oskolkov N, Johansson HJ, Guterstam P, Langel U. (2009). A stearylated CPP for delivery of splice correcting oligonucleotides using a non-covalent co-incubation strategy. J Control Release, 134, 221–227.

Morris VB, Sharma CP. (2011). Folate mediated l-arginine modified oligo (alkylaminosiloxane) graft poly (ethyleneimine) for tumor targeted gene delivery. Biomaterials, 32, 3030–3041.

Negishi Y, Endo Y, Fukuyama T, Suzuki R, Takizawa T, Omata D, Maruyama K, Aramaki Y. (2008). Delivery of siRNA into the cytoplasm by liposomal bubbles and ultrasound. J Control Release, 132, 124–130.

Negishi Y, Omata D, Iijima H, Hamano N, Endo-Takahashi Y, Nomizu M, Aramaki Y. (2010a). Preparation and characterization of laminin-derived peptide AG73-coated liposomes as a selective gene delivery tool. Biol Pharm Bull, 33, 1766–1769.

Negishi Y, Omata D, Iijima H, Takabayashi Y, Suzuki K, Endo Y, Suzuki R, Maruyama K, Nomizu M, Aramaki Y. (2010b). Enhanced laminin-derived peptide AG73-mediated liposomal gene transfer by bubble liposomes and ultrasound. Mol Pharm, 7, 217–226.

Negishi Y, Matsuo K, Endo-Takahashi Y, Suzuki K, Matsuki Y, Takagi N, Suzuki R, Maruyama K, Aramaki Y. (2011). Delivery of an

angiogenic gene into ischemic muscle by novel bubble liposomes followed by ultrasound exposure. Pharm Res, 28, 712–719.

Ng QK, Sutton MK, Soonsawad P, Xing L, Cheng H, Segura T. (2009). Engineering clustered ligand binding into nonviral vectors: alphavbeta3 targeting as an example. Mol Ther, 17, 828–836.

Pelkmans L, Püntener D, Helenius A. (2002). Local actin polymerization and dynamin recruitment in SV40-induced internalization of caveolae. Science, 296, 535–539.

Shi G, Guo W, Stephenson SM, Lee RJ. (2002). Efficient intracellular drug and gene delivery using folate receptor-targeted pH-sensitive liposomes composed of cationic/anionic lipid combinations. J Control Release, 80, 309–319.

Shin J, Shum P, Thompson DH. (2003). Acid-triggered release via dePEGylation of DOPE liposomes containing acid-labile vinyl ether PEG-lipids. J Control Release, 91, 187–200.

Sonawane ND, Szoka FC Jr, Verkman AS. (2003). Chloride accumulation and swelling in endosomes enhances DNA transfer by polyamine-DNA polyplexes. J Biol Chem, 278, 44826–44831.

Subbarao NK, Parente RA, Szoka FC Jr, Nadasdi L, Pongracz K. (1987). pH-dependent bilayer destabilization by an amphipathic peptide. Biochemistry, 26, 2964–2972.

Sun JY, Anand-Jawa V, Chatterjee S, Wong KK. (2003). Immune responses to adeno-associated virus and its recombinant vectors. Gene Ther, 10, 964–976.

Suzuki R, Namai E, Oda Y, Nishiie N, Otake S, Koshima R, Hirata K, Taira Y, Utoguchi N, Negishi Y, Nakagawa S, Maruyama K. (2010). Cancer gene therapy by IL-12 gene delivery using liposomal bubbles and tumoral ultrasound exposure. J Control Release, 142, 245–250.

Taniyama Y, Tachibana K, Hiraoka K, Aoki M, Yamamoto S, Matsumoto K, Nakamura T, Ogihara T, Kaneda Y, Morishita R. (2002). Development of safe and efficient novel nonviral gene transfer using ultrasound: enhancement of transfection efficiency of naked plasmid DNA in skeletal muscle. Gene Ther, 9, 372–380.

Varga CM, Tedford NC, Thomas M, Klibanov AM, Griffith LG, Lauffenburger DA. (2005). Quantitative comparison of polyethylenimine formulations and adenoviral vectors in terms of intracellular gene delivery processes. Gene Ther, 12, 1023–1032.

Wadia JS, Stan RV, Dowdy SF. (2004). Transducible TAT-HA fusogenic peptide enhances escape of TAT-fusion proteins after lipid raft macropinocytosis. Nat Med, 10, 310–315.

Walker GF, Fella C, Pelisek J, Fahrmeir J, Boeckle S, Ogris M, Wagner E. (2005). Toward synthetic viruses: endosomal pH-triggered deshielding of targeted polyplexes greatly enhances gene transfer *in vitro* and *in vivo*. Mol Ther, 11, 418–425.

Wang LH, Rothberg KG, Anderson RG. (1993). Mis-assembly of clathrin lattices on endosomes reveals a regulatory switch for coated pit formation. J Cell Biol, 123, 1107–1117.

Yamano S, Dai J, Yuvienco C, Khapli S, Moursi AM, Montclare JK. (2011). Modified Tat peptide with cationic lipids enhances gene transfection efficiency via temperature-dependent and caveolae-mediated endocytosis. J Control Release, 152, 278–285.

Yoshida T, Oide N, Sakamoto T, Yotsumoto S, Negishi Y, Tsuchiya S, Aramaki Y. (2006). Induction of cancer cell-specific apoptosis by folate-labeled cationic liposomes. J Control Release, 111, 325–332.

Zalipsky S, Qazen M, Walker JA 2nd, Mullah N, Quinn YP, Huang SK. (1999). New detachable poly(ethylene glycol) conjugates: cysteine-cleavable lipopolymers regenerating natural phospholipid, diacyl phosphatidylethanolamine. Bioconjug Chem, 10, 703–707.

Zhang S, Xu Y, Wang B, Qiao W, Liu D, Li Z. (2004). Cationic compounds used in lipoplexes and polyplexes for gene delivery. J Control Release, 100, 165–180.

Zhou Y, Shi J, Cui J, Deng CX. (2008). Effects of extracellular calcium on cell membrane resealing in sonoporation. J Control Release, 126, 34–43.

HEPATOLOGY
Official Journal of the American Association for the Study of Liver Diseases
AASLD

Efficient Suppression of Murine Intracellular Adhesion Molecule-1 Using Ultrasound-Responsive and Mannose-Modified Lipoplexes Inhibits Acute Hepatic Inflammation

Keita Un,[1,2] Shigeru Kawakami,[1] Mitsuru Yoshida,[1] Yuriko Higuchi,[3] Ryo Suzuki,[4] Kazuo Maruyama,[4] Fumiyoshi Yamashita,[1] and Mitsuru Hashida[1,5]

Hepatitis is often associated with the overexpression of various adhesion molecules. In particular, intracellular adhesion molecule-1 (ICAM-1), which is expressed on hepatic endothelial cells (HECs) in the early stage of inflammation, is involved in serious illnesses. Therefore, ICAM-1 suppression in HECs enables the suppression of inflammatory responses. Here, we developed an ICAM-1 small interfering RNA (siRNA) transfer method using ultrasound (US)-responsive and mannose-modified liposome/ICAM-1 siRNA complexes (Man-PEG_{2000} bubble lipoplexes [Man-PEG_{2000} BLs]), and achieved efficient HEC-selective ICAM-1 siRNA delivery in combination with US exposure. Moreover, the sufficient ICAM-1 suppression effects were obtained via this ICAM-1 siRNA transfer *in vitro* and *in vivo*, and potent anti-inflammatory effects were observed in various types of inflammation, such as lipopolysaccharide, dimethylnitrosamine, carbon tetrachloride, and ischemia/reperfusion-induced inflammatory mouse models. *Conclusion*: HEC-selective and efficient ICAM-1 siRNA delivery using Man-PEG_{2000} BLs and US exposure enables suppression of various types of acute hepatic inflammation. This novel siRNA delivery method may offer a valuable system for medical treatment where the targeted cells are HECs. (HEPATOLOGY 2012;56:259-269)

Hepatitis resulting from conditions such as drug-induced hepatic inflammation and ischemia/reperfusion (IR)-induced liver injury followed by surgery is a major obstacle for medical treatment.[1,2] Moreover, it was reported that chronic hepatitis progresses to cirrhosis and liver cancer[3,4]; therefore, the prevention and early treatment of hepatitis are important for patients and medical professionals. Most drug-induced hepatitis is caused by nuclear factor-κB activation and proinflammatory cytokine production followed by various stimulations in medical treatments.[5] In IR-induced liver injury, a large amount of reactive oxygen species produced by IR stimulation is involved in the induction of inflammatory responses.[6] Although the mechanism for each inflammatory response is different, various adhesion molecules, such as vascular cell adhesion molecule (VCAM) and intracellular adhesion molecule (ICAM), are abundantly expressed on hepatic endothelial cells (HECs) in the early stage of inflammatory responses followed by various types of stimulation.[7] Among these, ICAM-1 is known as a major molecule that is highly involved in the adhesion, diapedesis, and tissue infiltration of leukocytes contributing to the deterioration in inflammatory responses.[8] During alcohol-

Abbreviations: ALT, alanine aminotransferase; AST, aspartate aminotransferase; BL, bubble lipoplex; CCl_4, carbon tetrachloride; DAPI, 4′,6-diamidino-2-phenylindole; DMN, dimethylnitrosamine; FITC, fluorescein isothiocyanate; H&E, hematoxylin and eosin; HEC, hepatic endothelial cell; ICAM, intracellular adhesion molecule; IFN-γ, interferon-γ; IL, interleukin; IR, ischemia/reperfusion; iv, intravenous; LPS, lipopolysaccharide; MCP-1, monocyte chemoattractant protein 1; MDA-5, melanoma differentiation-associated gene 5; mRNA, messenger RNA; RIG-1, retinoic acid-inducible gene 1; siRNA, small interfering ribonucleic acid; TLR, Toll-like receptor; TNF-α, tumor necrosis factor α; US, ultrasound.

From the [1]Department of Drug Delivery Research, Graduate School of Pharmaceutical Sciences, the [3]Institute for Innovative NanoBio Drug Discovery and Development, Graduate School of Pharmaceutical Sciences, and the [5]Institute for Integrated Cell-Material Sciences, Kyoto University, Kyoto, Japan; [2]The Japan Society for the Promotion of Science, Tokyo, Japan; and the [4]Department of Biopharmaceutics, School of Pharmaceutical Sciences, Teikyo University, Kanagawa, Japan.

Received August 25, 2011; accepted January 16, 2012.

Supported in part by the Programs for Promotion of Fundamental Studies in Health Sciences of the National Institute of Biomedical Innovation; by the Health and Labour Sciences Research Grants for Research on Noninvasive and Minimally Invasive Medical Devices from the Ministry of Health, Labour and Welfare of Japan; and by a Grant-in-Aid for Scientific Research on Innovative Areas from the Ministry of Education, Culture, Sports, Science and Technology of Japan.

induced liver injury, it was reported that ICAM-1 expression and the resultant leukocyte infiltration are involved in the deterioration of alcohol-induced liver injury.[9] Therefore, the suppression of inflammatory responses may be achieved by selective knockdown of ICAM-1 in HECs.

RNA interference is an important endogenous mechanism for gene regulation by cleaving specific messenger RNA (mRNA) possessing the complementary sequence using small interfering RNA (siRNA).[10,11] Although siRNA is a promising candidate for molecular therapy, an effective method for siRNA transfer into the cytoplasm of targeted cells *in vivo* is still being developed. The effective methods for *in vivo* siRNA delivery involve nonviral carriers, including liposomes, emulsions, micelles, and polymers.[12-18] However, because the nonviral carriers are taken up into the cells via endocytosis, degradation within endosomes and escape from endosomes are major obstacles for the improvement of siRNA therapeutics. Moreover, efficient and selective siRNA delivery into HECs is essential to achieve the potent anti-inflammatory effects produced by ICAM-1 siRNA.

Recently, the benefits have become appreciated of delivery of nucleic acids into cells using microbubbles and ultrasound (US) (also known as "sonoporation methods"), due to the high transfer efficiency into the cytoplasm.[19-22] Our group has developed US-responsive and mannose-modified liposomes/plasmid DNA complexes for *in vivo* gene transfer and successfully obtained efficient gene expression in mannose receptor-expressing cells, such as HECs and splenic dendritic cells.[23-25] Moreover, we demonstrated that a large amount of plasmid DNA could be directly transferred into the cytoplasm through a mechanism involving transient pores created on the cell membrane by the destruction of microbubbles after US exposure.[26] Therefore, the efficient transfer of ICAM-1 siRNA into HECs might be achieved by applying this method to siRNA delivery.

In the present study, we developed an ICAM-1 siRNA transfer system based on US-responsive and mannose-modified liposome/siRNA complexes (Man-PEG_{2000} bubble lipoplexes [Man-PEG_{2000} BLs]) for anti-inflammatory therapy. ICAM-1 siRNA delivered by Man-PEG_{2000} BLs and US exposure was selectively and efficiently transferred into HECs *in vitro* and *in vivo*. Furthermore, sufficient ICAM-1 suppression and potent anti-inflammatory effects were achieved by ICAM-1 siRNA transfer against various types of inflammation induced by lipopolysaccharide (LPS), dimethylnitrosamine (DMN), carbon tetrachloride (CCl_4), and IR. To our knowledge, this is the first report of a gene transfer method using Man-PEG_{2000} BLs and US exposure for the selective and efficient transfer of siRNA to HECs. This novel siRNA transfer method could be valuable for medical treatments that target HECs.

Materials and Methods

In vitro *siRNA Delivery*. After incubation of HECs for 72 hours, the culture medium was replaced with Opti-MEM I (Invitrogen, Carlsbad, CA) containing lipoplexes/BLs (1 μg siRNA). At 5 minutes after siRNA transfer, HECs were exposed to US (frequency, 2.062 MHz; duty, 50%; burst rate, 10 Hz; intensity, 4.0 W/cm^2) for 20 seconds. In the siRNA delivery using naked siRNA and conventional nanobubbles, at 5 minutes after addition of naked siRNA (1 μg) and conventional nanobubbles (60 μg total lipids), cells were immediately exposed to US. US was generated using a Sonopore-4000 sonicator (Nepa Gene, Chiba, Japan). At 1 hour after US exposure, the medium was replaced with RPMI-1640 and incubated for an additional 23 hours. Lipofectamine 2000 (Invitrogen) was used according to the recommended procedures with an exposure time of 1 hour, which is the same exposure time in other experiments using lipoplexes.

In Vivo *siRNA Delivery*. Six-week-old C57BL/6 female mice were intravenously injected with BLs containing 10 μg siRNA via the tail vein. At 5 minutes after the injection of the bubble lipoplexes, US (frequency, 1.045 MHz; duty, 50%; burst rate, 10 Hz; intensity 1.0 W/cm^2; time, 2 minutes) was applied transdermally to the abdominal area using a Sonopore-4000 sonicator. In the siRNA delivery using naked siRNA and conventional nanobubbles, at 4 minutes after intravenous injection of conventional nanobubbles (500 μg total lipid), naked siRNA (10 μg) was intravenously injected and US was exposed at 1 minute after naked siRNA injection.

Address reprint requests to: Mitsuru Hashida, Ph.D., and Shigeru Kawakami, Ph.D. Department of Drug Delivery Research, Graduate School of Pharmaceutical Sciences, Kyoto University, 46-29 Yoshida-shimoadachi-cho, Sakyo-ku, Kyoto 606-8501, Japan. E-mail: hashidam@pharm.kyoto-u.ac.jp (Mitsuru Hashida) and kawakami@pharm.kyoto-u.ac.jp (Shigeru Kawakami); fax: (81)-75-753-4575.

View this article online at wileyonlinelibrary.com.

DOI 10.1002/hep.25607

Potential conflict of interest: Nothing to report.

Additional Supporting Information may be found in the online version of this article.

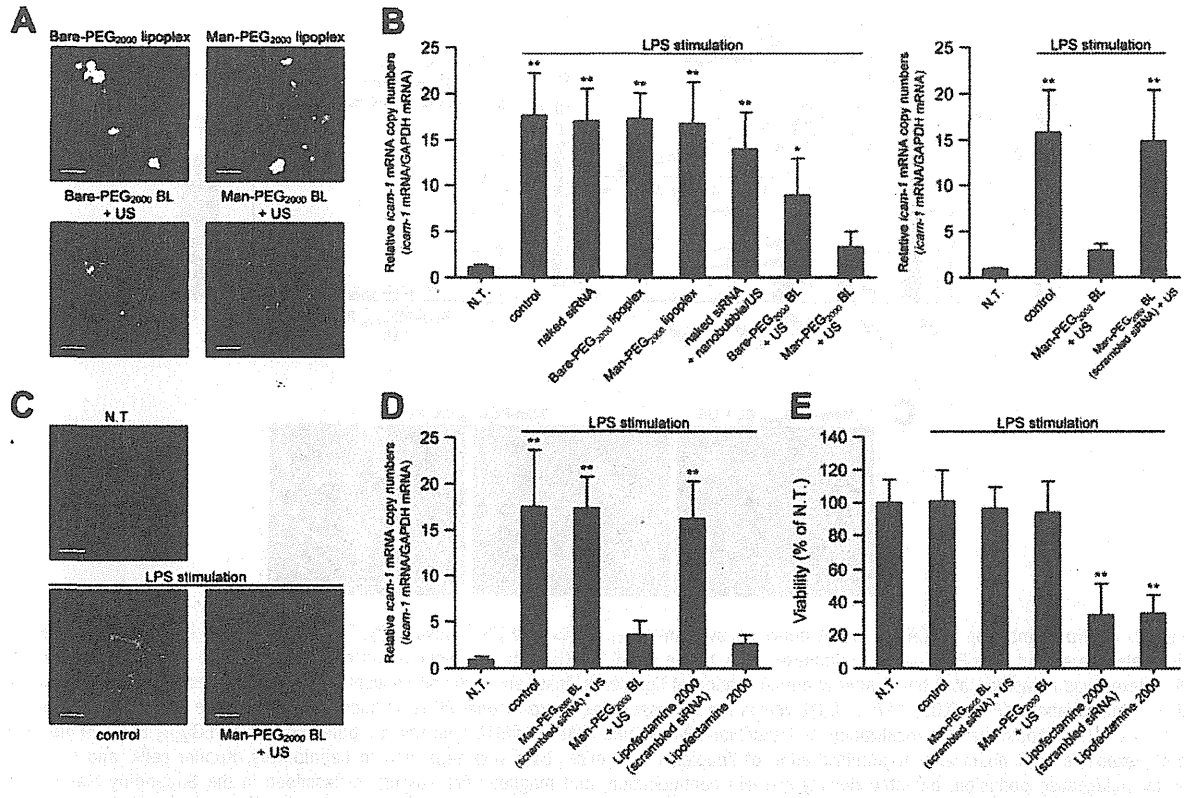

Fig. 1. Suppression effects of *icam-1* mRNA expression and cytotoxicity followed by ICAM-1 siRNA delivery in LPS-stimulated primary mouse HECs. (A) *In vitro* confocal images of cellular associated ICAM-1 siRNA (1 μg siRNA) transferred by various methods 1 hour after treatment in primary mouse HECs. US was directly exposed to HECs at 5 minutes after addition of BLs. The lipoplexes were constructed with AlexaFluor-594-labeled ICAM-1 siRNA (red), and the endosomes were labeled with AlexaFluor-488 transferrin conjugates (green). Nuclei were counterstained with 4′,6-diamidino-2-phenylindole (DAPI) (blue). Scale bars, 10 μm. (B,C) The level of *icam-1* mRNA expression (B) and *in vitro* confocal images of ICAM-1 expression (C) obtained by ICAM-1 siRNA transfer (1 μg siRNA) using various types of methods 24 hours after LPS stimulation in primary mouse HECs. US was directly exposed to HECs at 5 minutes after addition of BLs, and cells were exposed to LPS (100 ng/mL) at 24 hours after the addition of siRNA or lipoplexes/BLs. ICAM-1 was labeled with anti-mouse ICAM-1 antibody and fluorescein isothiocyanate (FITC)-conjugated secondary antibody (green), and nuclei were counterstained by DAPI (blue). Scale bars, 10 μm. (D,E) Comparison of the suppression of *icam-1* mRNA expression (D) and cell viability (E) obtained by siRNA transfer using Man-PEG_{2000} BLs (1 μg siRNA) and US exposure with that by Lipofectamine 2000. $^*P < 0.05$, $^{**}P < 0.01$ versus no treatment. Each value represents the mean + SD (n = 5). N.T., no treatment.

Statistical Analyses. Results are presented as the mean ± SD of more than three experiments. Analysis of variance was used to test the statistical significance of differences among groups. Two-group comparisons were performed using the Student *t* test and multiple comparisons between control and other groups were performed using the Dunnett's test.

Results

Suppression Effects of ICAM-1 siRNA. The suppression of LPS-induced ICAM-1 expression by ICAM-1 siRNAs (Supporting Fig. 1A) was investigated in primary mouse HECs. As shown in Supporting Fig. 1B, the suppression of ICAM-1 was the highest in ICAM-1 siRNA with sequence 1, and not observed in scrambled siRNA. Therefore, ICAM-1 siRNA containing sequence 1 and scrambled siRNA were used in the following examinations.

Physicochemical Properties of Man-PEG_{2000} BLs. Following enclosure of US imaging gas into Man-PEG_{2000} BLs, lipoplexes became cloudy (data not shown) and the average particle size increased (Supporting Fig. 2A). Following gel electrophoresis experiments, the formation of siRNA complexes in BLs was confirmed (Supporting Fig. 2B). Moreover, ζ-potentials of BLs were lower than that of liposomes (Supporting Fig. 2A), suggesting that siRNA was attached to the surface of cationic bubble liposomes. These physicochemical properties are consistent with our previous reports using plasmid DNA.[23-26]

Intracellular Transport Characteristics of ICAM-1 siRNA. The siRNA transfer efficiency was investigated in primary mouse HECs expressing mannose receptors (Supporting Fig. 4). The amount of siRNA delivered by BLs and US exposure was significantly higher than that by lipoplexes only (Supporting Fig. 3A).

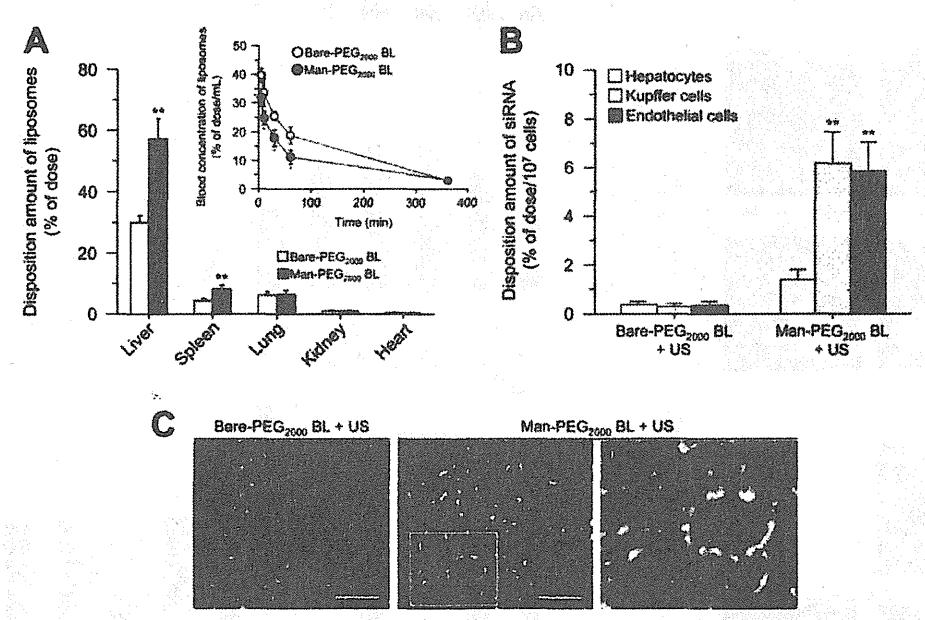

Fig. 2. *In vivo* distribution of ICAM-1 siRNA delivered by Man-PEG_{2000} BLs and US exposure. (A) Tissue distribution and pharmacokinetics of radiolabeled bare- and Man-PEG_{2000} BLs complexed with 10 μg ICAM-1 siRNA after intravenous (iv) administration into mice. Tissue distribution of lipoplexes was measured at 6 hours after iv administration of lipoplexes. Inset shows blood concentration of lipoplexes at predetermined times after iv administration. $^*P < 0.05$, $^{**}P < 0.01$ versus the corresponding group of bare-PEG_{2000} lipoplexes. Each value represents the mean $\pm$ SD ($n = 5$). (B) Hepatic cellular localization of AlexaFluor-594 labeled ICAM-1 siRNA delivered by bare- and Man-PEG_{2000} BLs (10 μg siRNA) and US exposure at 6 hours after iv administration of lipoplexes into mice. Liver was separated to hepatocytes, Kupffer cells, and endothelial cells by collagenase perfusion, one-step density gradient centrifugation, and magnetic cell sorting as described in the Supporting Materials and Methods. $^{**}P < 0.01$ versus the corresponding group of hepatocytes. Each value represents the mean + SD ($n = 5$). (C) Fluorescent images of hepatic localization of AlexaFluor-594-labeled ICAM-1 siRNA (red) delivered by bare- and Man-PEG_{2000} BLs (10 μg siRNA) and US exposure. HECs were labeled with anti-mouse CD146 antibody and FITC-conjugated secondary antibody (green), and nuclei were counterstained with DAPI (blue). Livers were harvested at 6 hours after iv administration of lipoplexes into mice, and magnified images corresponding to the areas enclosed in boxes are shown in the inset (i). Scale bars, 100 μm.

Moreover, the amount of siRNA delivered by Man-PEG_{2000} BLs and US exposure was higher than unmodified BLs. However, the amount of siRNA was significantly suppressed in the presence of mannan but not suppressed in the presence of chlorpromazine, an endocytosis inhibitor (Supporting Fig. 3B,C). Confocal microscopy analysis of cells after siRNA transfer by bubble lipoplexes with US exposure revealed that siRNA was not colocalized in endosomes (Fig. 1A). These observations suggest that siRNA is directly transferred into the cytoplasm of targeted cells and is not mediated by endocytosis in this siRNA transfer method.

***Suppression Effects of LPS-Induced ICAM-1 Expression* In Vitro.** As shown in Fig. 1B,C, ICAM-1 expression induced by LPS stimulation was suppressed by approximately 80% in siRNA transfer using Man-PEG_{2000} BLs and US exposure. The suppression effect of ICAM-1 expression was not observed for scrambled siRNA. Moreover, this suppression effect was comparable to that by Lipofectamine 2000 (Fig. 1D) but with decreased cytotoxicity (Fig. 1E).

In Vivo *distribution of ICAM-1 siRNA*. We investigated the pharmacokinetic profiles and the tissue distribution of BLs after intravenous administration into mice. Compared with nonmodified BLs, the retention time of Man-PEG_{2000} BLs in the blood was reduced, and localization in both the liver and spleen were increased (Fig. 2A). Moreover, a large amount of ICAM-1 siRNA was distributed in HECs that abundantly express mannose receptors when delivered using Man-PEG_{2000} BLs and US exposure (Fig. 2B,C).

***Suppression Effects of Drug-Induced Hepatic ICAM-1 Expression* In Vivo.** The suppression of ICAM-1 expression by siRNA delivery was investigated in an LPS/D-galactosamine–induced acute hepatitis mouse model (Fig. 3A). As shown in Fig. 3B-D, ICAM-1 mRNA and protein levels in HECs induced by LPS/D-galactosamine stimulation were suppressed by approximately 80% using Man-PEG_{2000} BLs and US exposure. Moreover, ICAM-1 expression induced by CCl_4 and DMN stimulation was also significantly suppressed by the same ICAM-1 siRNA delivery system (Supporting Figs. 6B and 7B). The effects of siRNA dose on ICAM-1 suppression and the duration of ICAM-1 suppression were examined in an LPS/D-galactosamine-induced inflammatory mouse model. Following siRNA delivery using Man-

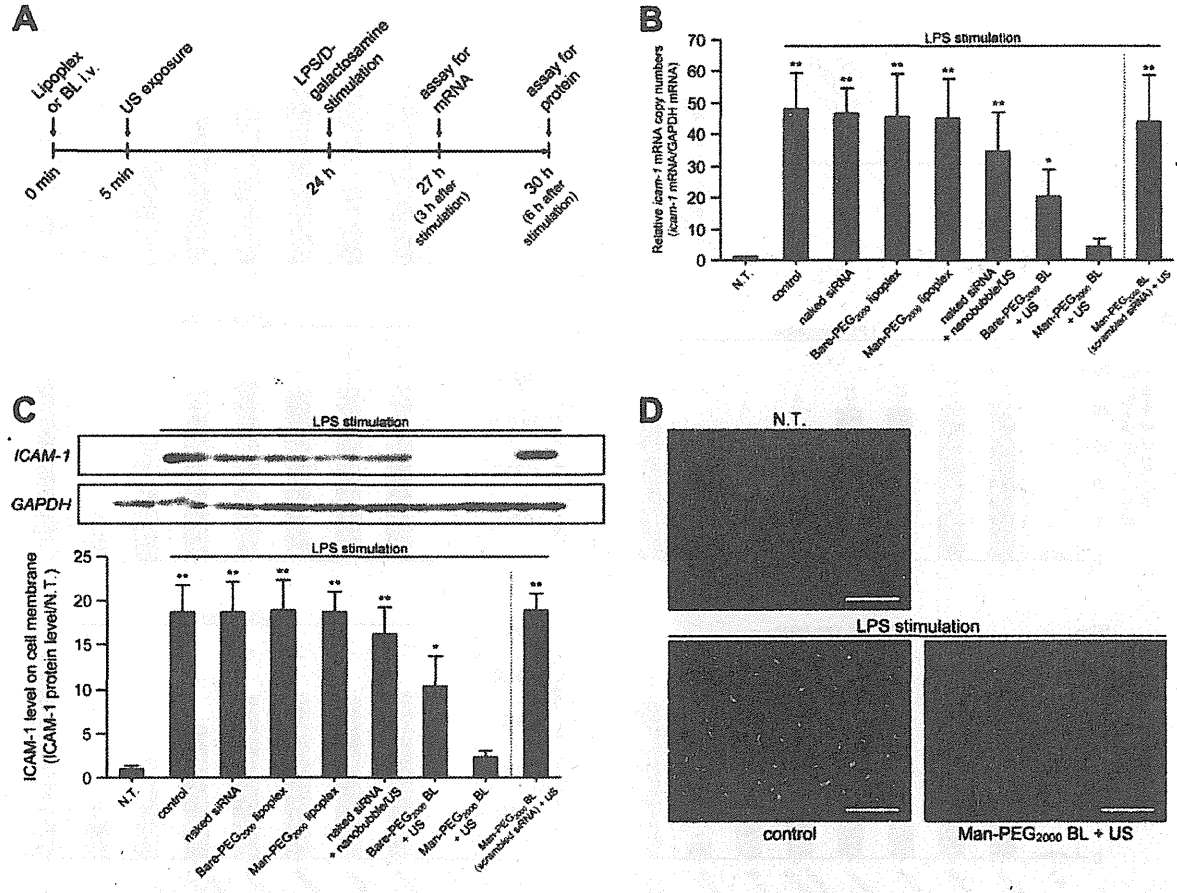

Fig. 3. Suppression effects of ICAM-1 siRNA delivery using Man-PEG_{2000} BLs and US exposure on *icam-1* mRNA and protein expression in HECs of an LPS/D-galactosamine-induced inflammatory mouse model. (A) Evaluation schedule of ICAM-1 expression in LPS/D-galactosamine-stimulated mice. (B-D) The expression level of *icam-1* mRNA in cells (B) and protein on the cell membrane (C, D) obtained by siRNA delivery (10 μg siRNA) using various methods in HECs. At 24 hours after siRNA delivery, LPS/D-galactosamine (1 μg/100 mg/kg) was intraperitoneally administered into mice to induce the acute inflammatory responses. HECs were isolated by collagenase perfusion, one-step density gradient centrifugation, and magnetic cell sorting as described in the Supporting Materials and Methods. The *icam-1* mRNA and protein expression in HECs was determined via quantitative reverse-transcription polymerase chain reaction (B), western blotting/enzyme-linked immunosorbent assay (C), and confocal images (D). The expression levels of mRNA and protein were detected at 3 and 6 hours after LPS/D-galactosamine stimulation, respectively. $^*P < 0.05$, $^{**}P < 0.01$ versus no treatment. Each value represents the mean + SD (n = 5). ICAM-1 was labeled with anti-mouse ICAM-1 antibody and FITC-conjugated secondary antibody (green), and nuclei were counterstained with DAPI (blue). Scale bars, 100 μm. N.T., no treatment.

PEG_{2000} BLs and US exposure, suppression was obtained at 10 μg of ICAM-1 siRNA (Supporting Fig. 5A), and was sustained for at least 3 days (Supporting Fig. 5B).

Anti-inflammatory Effects Against Drug-Induced Hepatitis. First, the suppression of leukocyte infiltration by ICAM-1 siRNA delivery was evaluated in an LPS/D-galactosamine–induced inflammatory mouse model (Fig. 4A). As shown in Fig. 4B,D, the expression of interleukin (IL)-8 and monocyte chemotactic protein 1 (MCP-1) was suppressed, and a significantly decreased number of infiltrated leukocytes were detected after siRNA delivery using Man-PEG_{2000} BLs and US exposure. Moreover, the production of proinflammatory cytokines (tumor necrosis factor α [TNF-α], interferon-γ [IFN-γ], and IL-6) were also suppressed by this siRNA delivery (Fig. 4C).

The anti-inflammatory effects obtained by ICAM-1 siRNA delivery were investigated next. As shown in Fig. 5A, alanine aminotransferase (ALT)/aspartate aminotransferase (AST) activities in the serum were markedly suppressed by siRNA delivery using Man-PEG_{2000} BLs and US exposure (Fig. 5A). As shown in Fig. 5B, hepatic apoptosis induced by LPS/D-galactosamine stimulation was significantly suppressed by this ICAM-1 siRNA delivery. Moreover, we performed hematoxylin and eosin (H&E) staining of liver sections to evaluate the effects on hepatic structural features. Although the circular and tube formations of the hepatic central vein were observed in normal liver section (Fig. 5C, left), they were crushed in the LPS-stimulated liver section (Fig. 5C, middle). On the other hand, destruction of the hepatic central vein induced by

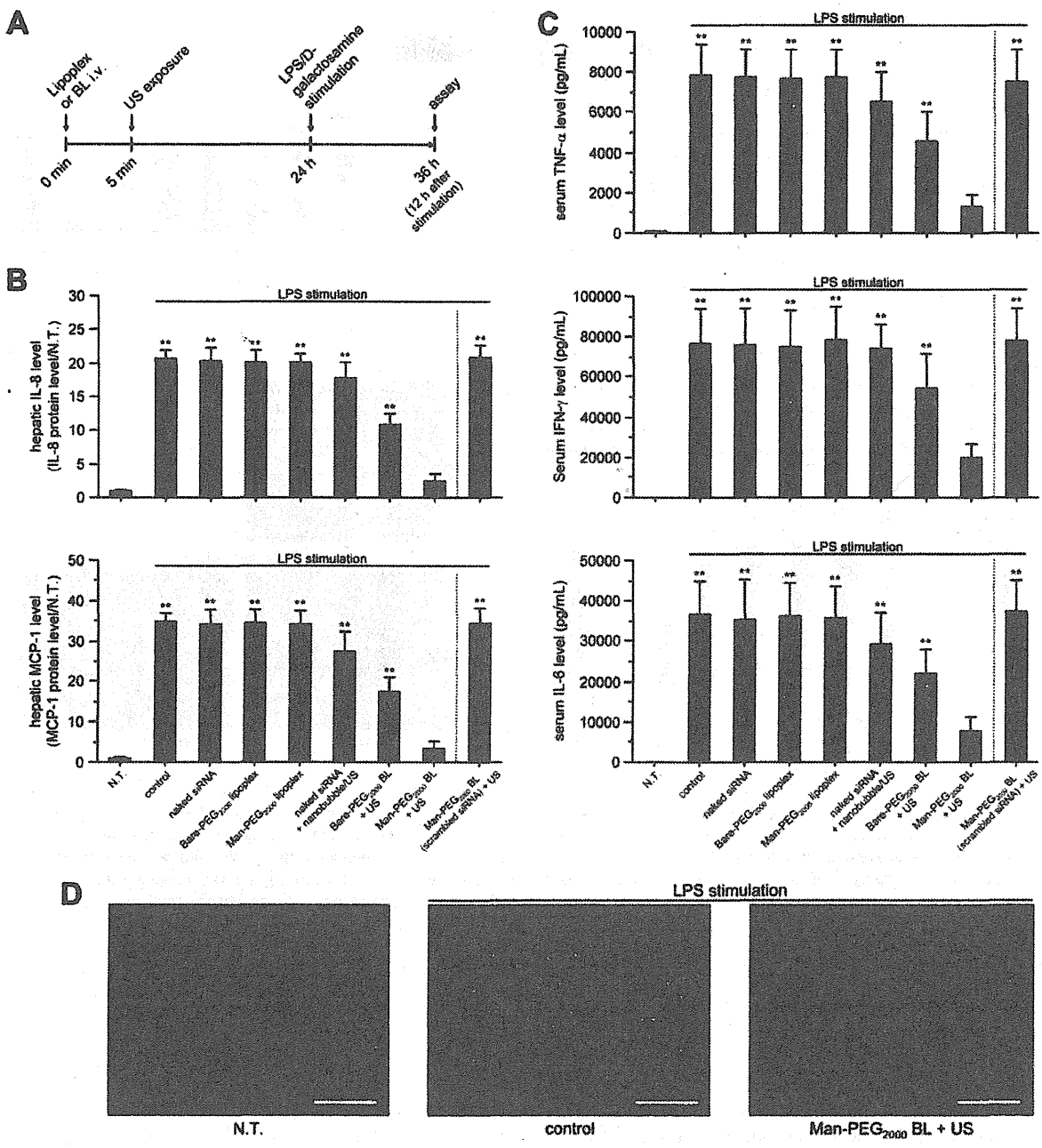

Fig. 4. Suppression effects of ICAM-1 siRNA delivery using Man-PEG_{2000} BLs and US exposure on leukocyte infiltration and proinflammatory cytokine production in an LPS/D-galactosamine-induced inflammatory mouse model. (A) Evaluation schedule of leukocyte infiltration and proinflammatory cytokine production in LPS/D-galactosamine-stimulated mice. (B,C) Levels of IL-8 and MCP-1 expression in the liver (B) and the levels of TNF-α, IFN-γ, and IL-6 secretion in the serum (C) after siRNA delivery (10 μg siRNA) using various delivery methods 12 hours after LPS/D-galactosamine stimulation. $^{**}P < 0.01$ versus no treatment. Each value represents the mean + SD (n = 5). N.T., no treatment. (D) Photomicrographs of infiltrated leukocytes after siRNA delivery using Man-PEG_{2000} BLs (10 μg siRNA) and US exposure in LPS/D-galactosamine-stimulated mouse liver. Leukocytes were labeled with anti-mouse Gr-1 (Ly-6G) antibody and rhodamine isothiocyanate-conjugated secondary antibody (red), and nuclei were counterstained with DAPI (blue). Scale bars, 100 μm. $^{**}P < 0.01$ versus no treatment. Each value represents the mean + SD (n = 5). N.T., no treatment.

LPS stimulation was significantly suppressed by ICAM-1 siRNA delivery using Man-PEG_{2000} BLs and US exposure (Fig. 5C, right), suggesting that the liver injury induced by LPS-stimulation is suppressed by this siRNA delivery. Similar effects by this ICAM-1 siRNA delivery were also observed for CCl_4- and DMN-induced inflammatory mouse models (Supporting Figs. 6C,D and 7C,D).

Anti-inflammatory Effects Against IR-Induced Liver Injury. The effects of ICAM-1 suppression by delivery of siRNA was evaluated for IR-induced liver

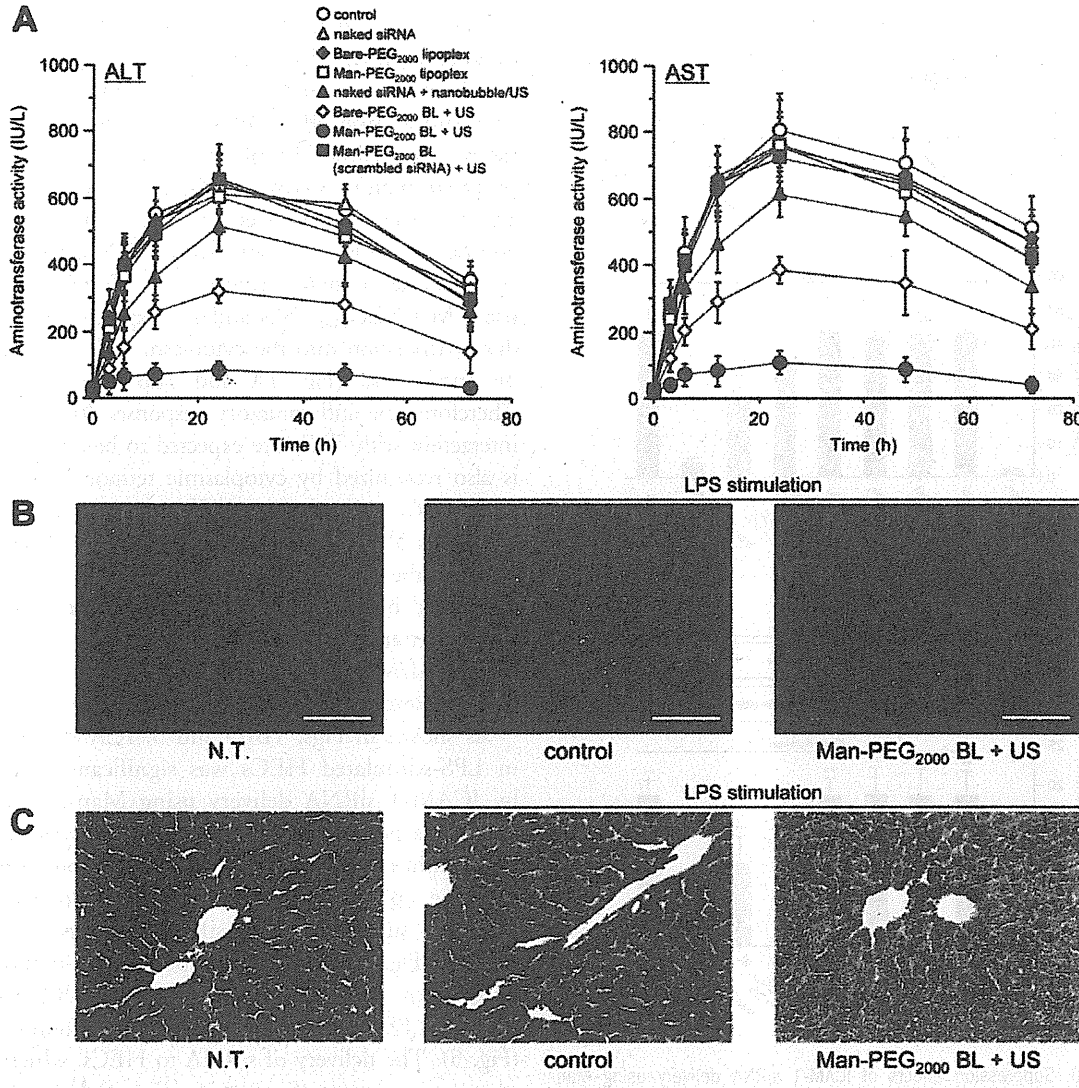

Fig. 5. Suppression effects of ICAM-1 siRNA delivery using Man-PEG_{2000} BLs and US exposure on liver toxicity in an LPS/D-galactosamine-induced inflammatory mouse model. (A) The level of serum ALT/AST activities after siRNA delivery (10 μg siRNA) using various methods at predetermined times after LPS/D-galactosamine stimulation. Each value represents the mean ± SD (n = 5). (B) Fluorescent images of apoptosis after siRNA delivery using Man-PEG_{2000} BLs (10 μg siRNA) and US exposure in LPS/D-galactosamine-stimulated mice. Apoptosis (green) was detected via terminal deoxynucleotidyl transferase-mediated deoxyuridine triphosphate nick-end labeling, and nuclei were counterstained with DAPI (blue). Scale bars, 100 μm. (C) Liver histology with H&E staining 24 hours after siRNA delivery using Man-PEG_{2000} BLs (10 μg siRNA) and US exposure in LPS/D-galactosamine-induced inflammatory mouse model. Black arrows: destruction of tube formation in hepatic central vein. Scale bars, 100 μm.

injury (Fig. 6A). As shown in Fig. 6B,C, ICAM-1 expression induced by IR stimulation was suppressed by siRNA delivery using Man-PEG_{2000} BLs and US exposure. Moreover, IL-8/MCP-1 expression and proinflammatory cytokine production were also suppressed (Fig. 7B,C). Following the examination of liver toxicity, ALT/AST activities in the serum and hepatic apoptosis were significantly suppressed (Fig. 8A,B). Moreover, after H&E staining of liver sections, the circular and tube formations of hepatic central vein in the normal liver (Fig. 8C, left) section is destructed by IR stimulation (Fig. 8C, middle), on the other hand, IR-derived destruction of hepatic central vein was suppressed by this ICAM-1 siRNA delivery (Fig. 5C, right).

Discussion

In the sonoporation method, transient pores are created on the cell membrane followed by the destruction of microbubbles, and a large amount of nucleic acids can be directly transferred into the cytoplasm.[21,26,27] Because siRNA is functionalized in the cytoplasm, gene

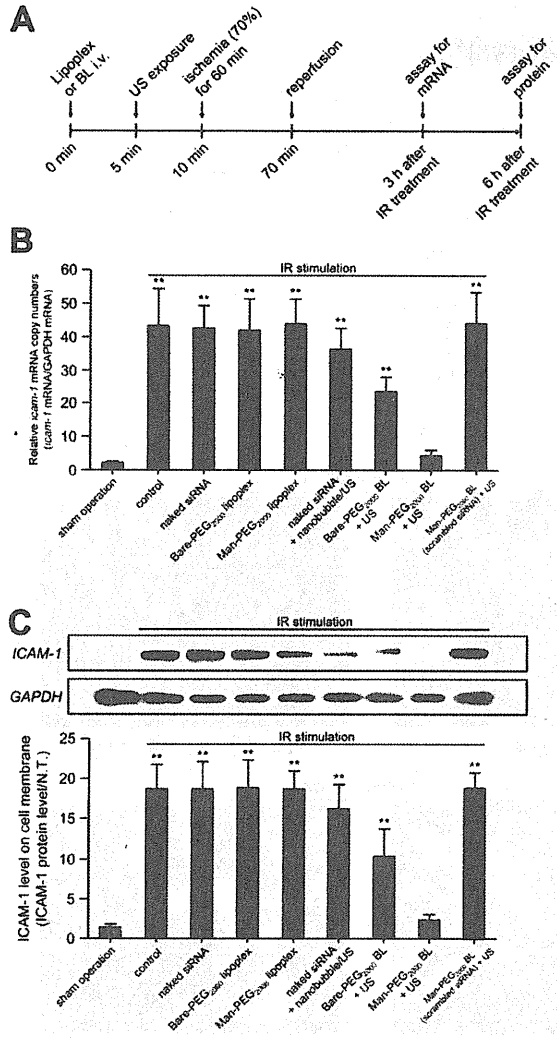

Fig. 6. Suppression effects of ICAM-1 siRNA delivery using Man-PEG_{2000} BLs and US exposure on *icam-1* mRNA and protein expression in HECs of an IR-induced hepatic inflammatory mouse model. (A) Evaluation schedule of ICAM-1 expression in hepatic IR-stimulated mice. (B,C) Expression level of *icam-1* mRNA in cells (B) and protein on the cell membrane (C) obtained by siRNA delivery (10 μg siRNA) using various delivery methods in HECs. HECs were isolated via collagenase perfusion, one-step density gradient centrifugation, and magnetic cell sorting as described in the Supporting Materials and Methods. The *icam-1* mRNA and protein expression in HECs was determined via quantitative reverse-transcription polymerase chain reaction (B) and western blotting/enzyme-linked immunosorbent assay (C). Expression levels of mRNA and protein were detected at 3 and 6 hours after IR stimulation, respectively. $^{*}P < 0.05$, $^{**}P < 0.01$ versus sham operation. Each value represents the mean + SD (n = 5).

transfer using Man-PEG_{2000} BLs and US exposure[23-26] would be also suitable for siRNA delivery. In the present study, we applied this gene transfer method for the selective and efficient delivery of siRNA to HECs *in vivo* and investigated the anti-inflammatory effects in various types of inflammatory responses.

The innate inflammatory responses based on the interaction with siRNA and Toll-like receptor (TLR)-3, -7, and -8 should be excluded for evaluating the gene suppression effects of siRNA, but should be considered for clinical applications of siRNA.[28,29] The proinflammatory cytokines (such as TNF-α, IFN-γ, and IL-6) can be induced by siRNA interaction with endosomal TLR-3, -7, and -8 in siRNA transfer using conventional nonviral carriers.[28,29] Transfer of siRNA using Man-PEG_{2000} BLs and US exposure results in the direct deposition into the cytoplasm and is not mediated by endocytosis (Fig. 1A and Supporting Fig. 3C).[26] Therefore, the inflammatory responses followed by the interaction with TLRs are expected to be low, but siRNA is also recognized by cytoplasmic retinoic acid-inducible gene 1 (RIG-1)/melanoma differentiation-associated gene 5 (MDA-5) involved in inflammatory responses.[28,30] Because the modification of 3′-overhang sequences is suppressed by the activation of interferon-responsive factors 3/7, transcriptional factors that exist downstream of the RIG-1/MDA-5 pathway,[31,32] we used siRNAs with 3′-dTdT overhang sequences (Supporting Fig. 1A).

As shown in Figs. 1B-D and 3, ICAM-1 expression in LPS-stimulated HECs was significantly suppressed by ICAM-1 siRNA delivery using Man-PEG_{2000} BLs and US exposure, both *in vitro* and *in vivo*. Similarly, tissue infiltration of leukocytes and proinflammatory cytokine production were both suppressed after ICAM-1 suppression by siRNA delivery using this method (Fig. 4). Furthermore, potent anti-inflammatory effects were obtained by this ICAM-1 siRNA delivery in an LPS-stimulated inflammatory mouse model (Fig. 5). The delivery of siRNA to HECs, which express mannose receptors (Supporting Fig. 4),[33] was selective and efficient using Man-PEG_{2000} BLs with US exposure (Fig. 2B,C). Moreover, because a large amount of siRNA was directly transferred into the cytoplasm (Fig. 1A and Supporting Fig. 3C),[26] endosomal escape and degradation within endosomes could be evaded. These data may indicate that nucleic acid transfer using Man-PEG_{2000} BLs and US exposure can be applied for siRNA delivery.

Although LPS is widely used to evaluate the induction of acute inflammatory responses, they are induced by not only various medicines but also surgical operations.[34] Aiming for the clinical application of anti-inflammatory therapy using our siRNA delivery method, the anti-inflammatory effects against various inflammatory models in mice were investigated. After evaluation of the anti-inflammatory effects against CCl_4-, DMN-, and IR-stimulated inflammation, ICAM-1 expression in HECs and the inflammatory responses was significantly suppressed by ICAM-1

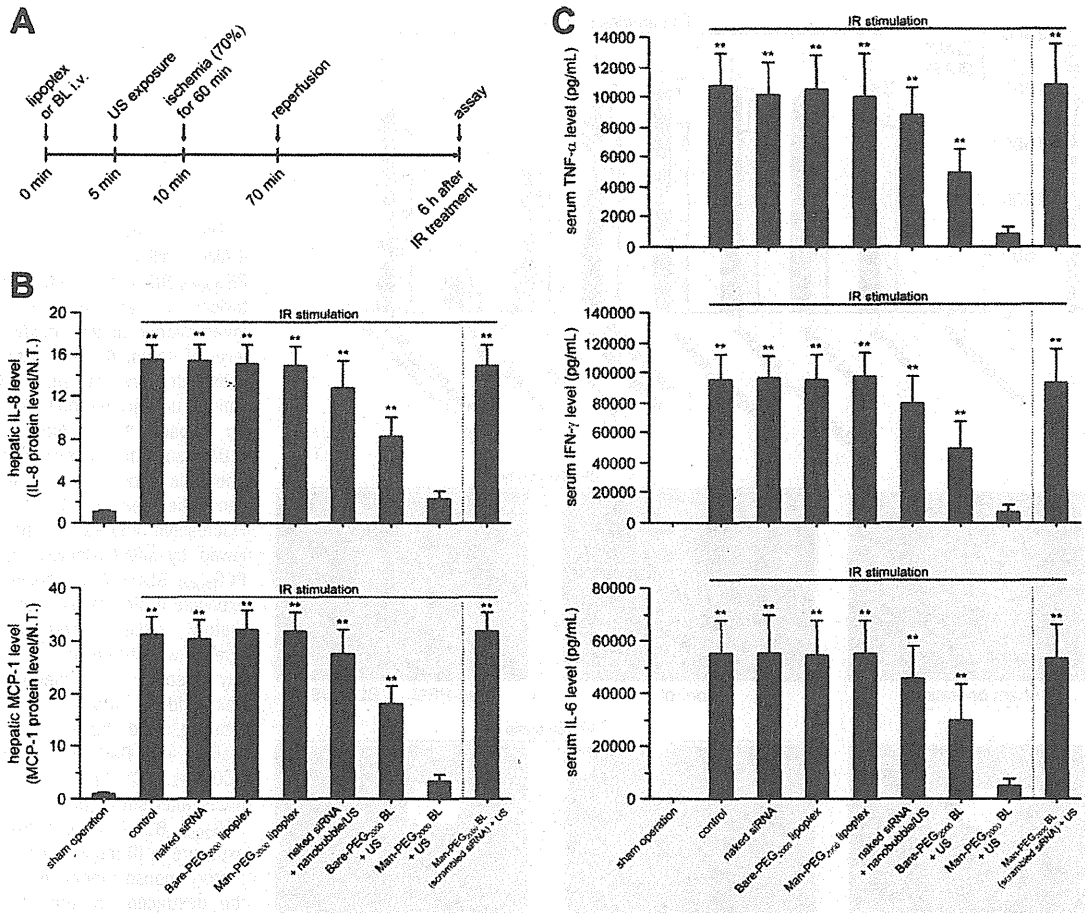

Fig. 7. Suppression effects of ICAM-1 siRNA delivery using Man-PEG_{2000} BLs and US exposure on leukocyte infiltration and proinflammatory cytokine production in IR-induced hepatic inflammatory mouse model. (A) Evaluation schedule of leukocyte infiltration and proinflammatory cytokine production in hepatic IR-stimulated mice. (B,C) Levels of IL-8 and MCP-1 expression in the liver (B) and TNF-α, IFN-γ, IL-6 secretion in the serum (C) after siRNA delivery (10 μg siRNA) using various delivery methods 6 hours after IR stimulation. $^{**}P < 0.01$ versus sham operation. Each value represents the mean + SD (n = 5).

siRNA delivery using Man-PEG_{2000} BLs and US exposure in these inflammatory mouse models (Figs. 6-8 and Supporting Figs. 6 and 7). Although the mechanisms of inflammatory responses as a result of LPS, CCl_4, DMN, and IR stimulation are different,[5,6,35,36] ICAM-1 expression in HECs is reported in various types of inflammation, including drug-induced hepatic inflammation and IR-induced liver injury.[7] These data suggest that anti-inflammatory effects obtained by ICAM-1 siRNA delivery using Man-PEG_{2000} BLs and US exposure may be beneficial for acute hepatitis and liver injury.

In the present study, efficient ICAM-1 suppression was obtained at a dose of 1 μg siRNA/mouse (0.05 mg/kg) for siRNA delivery using Man-PEG_{2000} BLs and US exposure *in vivo* (Supporting Fig. 5A). This dose of siRNA is lower than those reported for other studies evaluating the therapeutic effects using siRNA, although the therapeutic mechanism and delivery methods of each siRNA are likely to be different.[37-39] These findings suggest that the increased distribution of siRNA into HECs by mannose modification (Fig. 2) and the enhancement of intracytoplasmic siRNA transfer by sonoporation (Fig. 1A and Supporting Fig. 3) could contribute to the potent anti-inflammatory effects observed at a low dose of siRNA in our siRNA delivery method.

ICAM-1 suppression effects were only sustained for 72 hours by siRNA delivery using Man-PEG_{2000} BLs and US exposure (Supporting Fig. 5B). However, because the disease target of this study was acute inflammation, the potent therapeutic effects might be obtained in short duration and single administration of siRNA. Recently, it has been reported that ICAM-1 is involved in various diseases not only for acute/chronic hepatic failure, but also Crohn's disease, ulcerative colitis, and ileus.[40-42] In addition, antisense oligonucleotides against ICAM-1 (ISIS-2302; Alicaforsen)

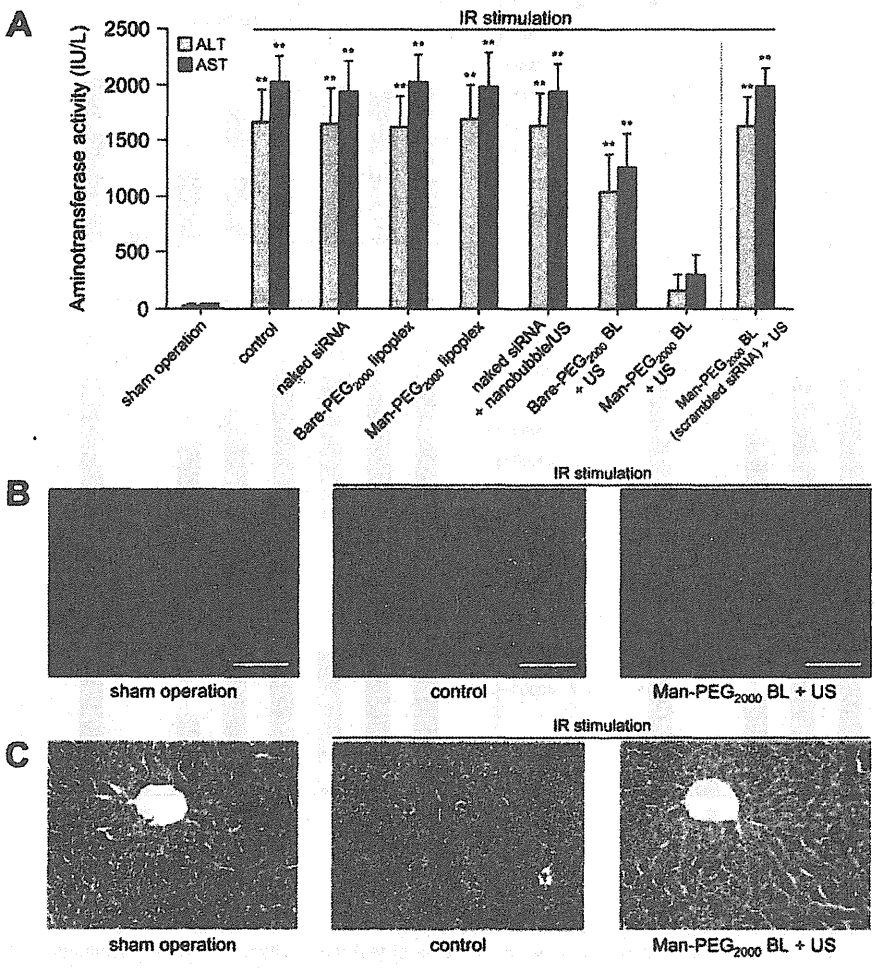

Fig. 8. Suppression effects of ICAM-1 siRNA delivery using Man-PEG_{2000} BLs and US exposure on liver toxicity in an IR-induced hepatic inflammatory mouse model. (A) The level of serum ALT/AST activities after siRNA delivery (10 μg siRNA) using various delivery methods 24 hours after hepatic IR stimulation. $^{**}P <$ 0.01versus the corresponding sham operation group. Each value represents the mean + SD (n = 5). (B) Fluorescent images of apoptosis followed by siRNA delivery using Man-PEG_{2000} BLs (10 μg siRNA) and US exposure in IR-induced hepatic inflammatory mouse model. Apoptosis (green) was detected via terminal deoxynucleotidyl transferase-mediated deoxyuridine triphosphate nick-end labeling, and nuclei were counterstained with DAPI (blue). Scale bars, 100 μm. (C) Liver histology at 24 hours after siRNA delivery using Man-PEG_{2000} BLs (10 μg siRNA) and US exposure in IR-induced hepatic inflammatory mouse model. Arrows indicate the destruction of tube formation in the hepatic central vein. Scale bars, 100 μm.

are currently under development for the treatment of Crohn's disease and ulcerative colitis.[43,44] However, most of these inflammatory diseases are based on chronic inflammation. In the present study, it is strongly suggested that transfer of ICAM-1 siRNA using Man-PEG_{2000} BLs and US exposure enables a large amount of siRNA to be delivered the cytoplasm of targeted cells (Fig. 1A and Supporting Fig. 3). Therefore, to prolong the duration of gene suppression using this siRNA delivery system, future studies using cholesterol-modified siRNA[45] or locked nucleic acid,[46] which are forms of stable siRNA resistant to enzymatic degradation, might be necessary for application to a variety of chronic inflammatory diseases.

In conclusion, ICAM-1 siRNA was transferred into HECs selectively and efficiently, and sufficient ICAM-1 suppression effects were obtained by ICAM-1 siRNA transfer using Man-PEG_{2000} BLs and US exposure, both *in vitro* and *in vivo*. Moreover, potent anti-inflammatory effects were achieved against various types of inflammation by this ICAM-1 siRNA transfer. These findings contribute to overcoming the poor efficiency of siRNA transfer into the cytoplasm of the targeted cells using nonviral carriers, and this novel siRNA delivery method using Man-PEG_{2000} BLs and US exposure may offer a valuable system for medical treatment where the cellular targets are HECs.

References

1. Verma S, Kaplowitz N. Diagnosis, management and prevention of drug-induced liver injury. Gut 2009;58:1555-1564.
2. Gurusamy KS, Gonzalez HD, Davidson BR. Current protective strategies in liver surgery. World J Gastroenterol 2010;16:6098-6103.
3. Freeman AJ, Dore GJ, Law MG, Thorpe M, Von Overbeck J, Lloyd AR, et al. Estimating progression to cirrhosis in chronic hepatitis C virus infection. HEPATOLOGY 2001;34:809-816.
4. Kuper H, Ye W, Broomé U, Romelsjö A, Mucci LA, Ekbom A, et al. The risk of liver and bile duct cancer in patients with chronic viral hepatitis, alcoholism, or cirrhosis. HEPATOLOGY 2001;34:714-718.
5. Tsuchiya H, Kaibori M, Yanagida H, Yokoigawa N, Kwon AH, Okumura T, et al. Pirfenidone prevents endotoxin-induced liver injury after partial hepatectomy in rats. J Hepatol 2004;40:94-101.
6. Teoh NC, Farrell GC. Hepatic ischemia reperfusion injury: pathogenic mechanisms and basis for hepatoprotection. J Gastroenterol Hepatol 2003;18:891-902.

7. Jaeschke H. Mechanisms of liver injury. II. Mechanisms of neutrophil-induced liver cell injury during hepatic ischemia-reperfusion and other acute inflammatory conditions. Am J Physiol Gastrointest Liver Physiol 2006;290:1083-1088.
8. Rijcken E, Krieglstein CF, Anthoni C, Laukoetter MG, Mennigen R, Spiegel HU, et al. ICAM-1 and VCAM-1 antisense oligonucleotides attenuate in vivo leucocyte adherence and inflammation in rat inflammatory bowel disease. Gut 2002;51:529-535.
9. Kono H, Uesugi T, Froh M, Rusyn I, Bradford BU, Thurman RG. ICAM-1 is involved in the mechanism of alcohol-induced liver injury: studies with knockout mice. Am J Physiol Gastrointest Liver Physiol 2001;280:G1289-G1295.
10. Elbashir SM, Lendeckel W, Tuschl T. RNA interference is mediated by 21- and 22-nucleotide RNAs. Genes Dev 2001;15:188-200.
11. Elbashir SM, Harborth J, Lendeckel W, Yalcin A, Weber K, Tuschl T. Duplexes of 21-nucleotide RNAs mediate RNA interference in cultured mammalian cells. Nature 2001;411:494-498.
12. Sato A, Takagi M, Shimamoto A, Kawakami S, Hashida M. Small interfering RNA delivery to the liver by intravenous administration of galactosylated cationic liposomes in mice. Biomaterials 2007;28:1434-1442.
13. Kawakami S, Hashida M. Targeted delivery systems of small interfering RNA by systemic administration. Drug Metab Pharmacokinet 2007;22:142-151.
14. Mok H, Lee SH, Park JW, Park TG. Multimeric small interfering ribonucleic acid for highly efficient sequence-specific gene silencing. Nat Mater 2010;9:272-278.
15. Kim SS, Ye C, Kumar P, Chiu I, Subramanya S, Wu H, et al. Targeted delivery of siRNA to macrophages for anti-inflammatory treatment. Mol Ther 2010;18:993-1001.
16. Davis ME, Zuckerman JE, Choi CH, Seligson D, Tolcher A, Alabi CA, et al. Evidence of RNAi in humans from systemically administered siRNA via targeted nanoparticles. Nature 2010;464:1067-1070.
17. Takemoto H, Ishii A, Miyata K, Nakanishi M, Oba M, Ishii T, et al. Polyion complex stability and gene silencing efficiency with a siRNA-grafted polymer delivery system. Biomaterials 2010;31:8097-8105.
18. Higuchi Y, Kawakami S, Hashida M. Strategies for in vivo delivery of siRNAs: recent progress. BioDrugs 2010;24:195-205.
19. Hernot S, Klibanov AL. Microbubbles in ultrasound-triggered drug and gene delivery. Adv Drug Deliv Rev 2008;60:1153-1166.
20. Li YS, Davidson E, Reid CN, McHale AP. Optimising ultrasound-mediated gene transfer (sonoporation) in vitro and prolonged expression of a transgene in vivo: potential applications for gene therapy of cancer. Cancer Lett 2009;273:62-69.
21. Lentacker I, Wang N, Vandenbroucke RE, Demeester J, De Smedt SC, Sanders NN. Ultrasound exposure of lipoplex loaded microbubbles facilitates direct cytoplasmic entry of the lipoplexes. Mol Pharm 2009;6:457-467.
22. Negishi Y, Matsuo K, Endo-Takahashi Y, Suzuki K, Matsuki Y, Takagi N, et al. Delivery of an angiogenic gene into ischemic muscle by novel bubble liposomes followed by ultrasound exposure. Pharm Res 2011; 28:712-719.
23. Un K, Kawakami S, Suzuki R, Maruyama K, Yamashita F, Hashida M. Development of an ultrasound-responsive and mannose-modified gene carrier for DNA vaccine therapy. Biomaterials 2010;31:7813-7826.
24. Un K, Kawakami S, Suzuki R, Maruyama K, Yamashita F, Hashida M. Suppression of melanoma growth and metastasis by DNA vaccination using an ultrasound-responsive and mannose-modified gene carrier. Mol Pharm 2011;8:543-554.
25. Un K, Kawakami S, Higuchi Y, Suzuki R, Maruyama K, Yamashita F, et al. Involvement of activated transcriptional process in efficient gene transfection using unmodified and mannose-modified bubble lipoplexes with ultrasound exposure. J Control Release 2011;156:355-363.
26. Un K, Kawakami S, Yoshida M, Higuchi Y, Suzuki R, Maruyama K, et al. The elucidation of gene transferring mechanism by ultrasound-responsive unmodified and mannose-modified lipoplexes. Biomaterials 2011;32:4659-4669.
27. Negishi Y, Endo Y, Fukuyama T, Suzuki R, Takizawa T, Omata D, et al. Delivery of siRNA into the cytoplasm by liposomal bubbles and ultrasound. J Control Release 2008;132:124-130.
28. Matsushima H, Yamada N, Matsue H, Shimada S. TLR3-, TLR7-, and TLR9-mediated production of proinflammatory cytokines and chemokines from murine connective tissue type skin-derived mast cells but not from bone marrow-derived mast cells. J Immunol 2004;173:531-541.
29. Kawai T, Akira S. Toll-like receptor and RIG-I-like receptor signaling. Ann N Y Acad Sci 2008;1143:1-20.
30. Matsukura S, Kokubu F, Kurokawa M, Kawaguchi M, Ieki K, Kuga H, et al. Role of RIG-I, MDA-5, and PKR on the expression of inflammatory chemokines induced by synthetic dsRNA in airway epithelial cells. Int Arch Allergy Immunol 2007;143:80-83.
31. Marques JT, Devosse T, Wang D, Zamanian-Daryoush M, Serbinowski P, Hartmann R, et al. A structural basis for discriminating between self and nonself double-stranded RNAs in mammalian cells. Nat Biotechnol 2006;24:559-565.
32. Sato Y, Murase K, Kato J, Kobune M, Sato T, Kawano Y, et al. Resolution of liver cirrhosis using vitamin A-coupled liposomes to deliver siRNA against a collagen-specific chaperone. Nat Biotechnol 2008;26: 431-442.
33. Elvevold K, Simon-Santamaria J, Hasvold H, McCourt P, Smedsrød B, Sørensen KK. Liver sinusoidal endothelial cells depend on mannose receptor-mediated recruitment of lysosomal enzymes for normal degradation capacity. HEPATOLOGY 2008;48:2007-2015.
34. Norris W, Paredes AH, Lewis JH. Drug-induced liver injury in 2007. Curr Opin Gastroenterol 2008;24:287-297.
35. Simeonova PP, Gallucci RM, Hulderman T, Wilson R, Kommineni C, Rao M, et al. The role of tumor necrosis factor-alpha in liver toxicity, inflammation, and fibrosis induced by carbon tetrachloride. Toxicol Appl Pharmacol 2001;177:112-120.
36. Oyaizu T, Shikata N, Senzaki H, Matsuzawa A, Tsubura A. Studies on the mechanism of dimethylnitrosamine-induced acute liver injury in mice. Exp Toxicol Pathol 1997;49:375-380.
37. Song E, Lee SK, Wang J, Ince N, Ouyang N, Min J, et al. RNA interference targeting Fas protects mice from fulminant hepatitis. Nat Med 2003;9:347-351.
38. Yano J, Hirabayashi K, Nakagawa S, Yamaguchi T, Nogawa M, Kashimori I, et al. Antitumor activity of small interfering RNA/cationic liposome complex in mouse models of cancer. Clin Cancer Res 2004;10: 7721-7726.
39. Zimmermann TS, Lee AC, Akinc A, Bramlage B, Bumcrot D, Fedoruk MN, et al. RNAi-mediated gene silencing in non-human primates. Nature 2006;441:111-114.
40. Yacyshyn BR, Schievella A, Sewell KL, Tami JA. Gene polymorphisms and serological markers of patients with active Crohn's disease in a clinical trial of antisense to ICAM-1. Clin Exp Immunol 2005;141:141-147.
41. Miner PB Jr, Geary RS, Matson J, Chuang E, Xia S, Baker BF, et al. Bioavailability and therapeutic activity of alicaforsen (ISIS 2302) administered as a rectal retention enema to subjects with active ulcerative colitis. Aliment Pharmacol Ther 2006;23:1427-1434.
42. The FO, Jonge WJ, Bennink RJ, van den Wijngaard RM, Boeckxstaens GE. The ICAM-1 antisense oligonucleotide ISIS-3082 prevents the development of postoperative ileus in mice. Br J Pharmacol 2005;146: 252-258.
43. Yacyshyn BR, Chey WY, Goff J, Salzberg B, Baerg R, Buchman AL, et al. Double blind, placebo controlled trial of the remission inducing and steroid sparing properties of an ICAM-1 antisense oligodeoxynucleotide, alicaforsen (ISIS 2302), in active steroid dependent Crohn's disease. Gut 2002;51:30-36.
44. van Deventer SJ, Tami JA, Wedel MK. A randomised, controlled, double blind, escalating dose study of alicaforsen enema in active ulcerative colitis. Gut 2004;53:1646-1651.
45. Ambardekar VV, Han HY, Varney ML, Vinogradov SV, Singh RK, Vetro JA. The modification of siRNA with 3′ cholesterol to increase nuclease protection and suppression of native mRNA by select siRNA polyplexes. Biomaterials 2011;32:1404-1411.
46. Elmén J, Thonberg H, Ljungberg K, Frieden M, Westergaard M, Xu Y, et al. Locked nucleic acid (LNA) mediated improvements in siRNA stability and functionality. Nucleic Acids Res 2005;33:439-447.

Journal of Controlled Release 160 (2012) 362–366

Contents lists available at SciVerse ScienceDirect

Journal of Controlled Release

journal homepage: www.elsevier.com/locate/jconrel

Prophylactic immunization with Bubble liposomes and ultrasound-treated dendritic cells provided a four-fold decrease in the frequency of melanoma lung metastasis

Yusuke Oda [a,1], Ryo Suzuki [a,1], Shota Otake [a,1], Norihito Nishiie [a], Keiichi Hirata [a], Risa Koshima [a], Tetsuya Nomura [a], Naoki Utoguchi [a], Nobuki Kudo [b], Katsuro Tachibana [c], Kazuo Maruyama [a,*]

[a] Department of Biopharmaceutics, School of Pharmaceutical Sciences, Teikyo University, Japan
[b] Laboratory of Biomedical Engineering, Graduate School of Information Science and Technology, Hokkaido University, Japan
[c] Department of Anatomy, School of Medicine, Fukuoka University, Japan

ARTICLE INFO

Article history:
Received 15 July 2011
Accepted 6 December 2011
Available online 13 December 2011

Keywords:
Dendritic cells
Antigen delivery system
Cancer immunotherapy
Ultrasound
Liposomes

ABSTRACT

Melanoma has an early tendency to metastasize, and the majority of the resulting deaths are caused by metastatic melanoma. It is therefore important to develop effective therapies for metastasis. Dendritic cell (DC)-based cancer immunotherapy has been proposed as an effective therapeutic strategy for metastasis and recurrence due to prime tumor-specific cytotoxic T lymphocytes. In this therapy, it is important that DCs present peptides derived from tumor-associated antigens on MHC class I molecules. Previously, we developed an innovative approach capable of directly delivering exogenous antigens into the cytosol of DCs using perfluoropropane gas-entrapping liposomes (Bubble liposomes, BLs) and ultrasound. In the present study, we investigated the prevention of melanoma lung metastasis via DC-based immunotherapy. Specifically, antigens were extracted from melanoma cells and used to treat DCs by BL and ultrasound. Delivery into the DCs by this route did not require the endocytic pathway. The delivery efficiency was approximately 74.1%. DCs treated with melanoma-derived antigens were assessed for *in vivo* efficacy in a mouse model of lung metastasis. Prophylactic immunization with BL/ultrasound-treated DCs provided a four-fold decrease in the frequency of melanoma lung metastases. These *in vitro* and *in vivo* results demonstrate that the combination of BLs and ultrasound is a promising method for antigen delivery system into DCs.

1. Introduction

Melanoma is the most devastating form of skin cancer and represents a leading cause of cancer death. Relative to the tumor mass, melanomas have an early tendency to metastasize; indeed, the majority of melanoma deaths are caused by metastatic disease. As a result, the prognosis for melanoma is poor. In fact, the 5-year survival rate of patients with localized melanoma is up to 90%; in contrast, patients with metastasized melanoma have 5-year survival rates of only 20% [1,2]. Additionally, melanoma is usually resistant to standard chemotherapy, and the response rate for any single agent or combination of agents ranges from 5% to 45% [3,4]. Based on these data, there is a clear need to develop effective therapy for metastasized melanoma. There are various therapeutic methods for metastatic cancer, such as surgical treatment, chemotherapy, radiotherapy, and immunotherapy. Of these methods, immunotherapy may be the most promising because of the possibility of preventing systemic metastasis and recurrence in the long term [5–9].

Dendritic cells (DCs), which are unique antigen-presenting cells capable of priming naive T cells, have been used as vaccine carriers for cancer immunotherapy [6,10]. To induce an effective tumor-specific cytotoxic T-lymphocyte (CTL) response, DCs should abundantly present epitope peptides derived from tumor-associated antigens (TAAs) via major histocompatibility complex (MHC) class I molecules and MHC class II molecules [11]. In general, exogenous antigens (such as TAAs in DCs) are preferentially presented on MHC class II molecules [12,13]. On the other hand, the majority of peptides presented via the MHC class I molecules are generated from endogenously synthesized proteins that are degraded by the proteasome [12]. Therefore, in order to efficiently prime TAA-specific CTLs, it is necessary to develop a novel antigen delivery system that can induce MHC class I-restricted TAA presentation on DCs. Several researchers have studied antigen delivery tools based on the cross-presentation theory of exogenous antigens in DCs [14–19]. Proposed antigen delivery carriers have included liposomes [15,16], poly(γ-glutamic acid) nanoparticles [17], and cholesterol pullulan nanoparticles [18]. All of these carriers deliver the antigens into DCs via the endocytic pathway, inducing the leaking of exogenous antigens from the endosome into the cytosol. Finally, it is thought that the antigens leaked into the cytosol are

Abbreviations: BL, Bubble liposome; CTL, cytotoxic T-lymphocyte; DC, dendritic cell; FITC, fluorescein isothiocyanate; MHC, major histocompatibility complex; MW, molecular weight; PBS, phosphate-buffered saline; TAA, tumor-associated antigen; US, ultrasound.

* Corresponding author at: Department of Biopharmaceutics, School of Pharmaceutical Sciences, Teikyo University, 1091-1 Suwarashi, Midori-ku, Sagamihara, Kanagawa 252-5195, Japan. Tel.: +81 42 685 3722; fax: +81 42 685 3432.
E-mail address: maruyama@pharm.teikyo-u.ac.jp (K. Maruyama).
[1] These authors contributed equally to this work.

0168-3659/$ – see front matter.
doi:10.1016/j.jconrel.2011.12.003

presented on MHC class I molecules. As an alternative, we have sought to use an antigen delivery system that does not rely on the endocytic pathway.

Multiple papers have reported the use of microbubbles for ultrasound-mediated gene and drug delivery [20–26]. In this delivery system, microstreams and microjets, which are induced by disruption of nano/microbubbles exposed to ultrasound, promote the transfer of extracellular materials into cells by opening transient pores in the cell membrane [27,28]. Previously, we described ultrasound-mediated antigen delivery in DCs using Bubble liposomes (BLs) containing perfluoropropane, an ultrasound imaging gas [29]. Using this system, a model antigen (ovalbumin) could be delivered into the cytosol of DCs independent of the endocytic pathway. This technique provided direct entry of the exogenous antigens into the MHC class I presentation pathway, resulting in the priming of exogenous antigen-specific CTLs. We proposed that this system could facilitate the delivery of crude antigens (such as tumor lysates and extracts) because such substrates could enter cells via a transient pore. In the present study, we used fluorescein isothiocyanate (FITC)-dextran as a substrate to characterize antigen delivery by BLs and ultrasound. Additionally, we assessed the possible application of BLs and ultrasound in DC-based immunotherapy in an *in vivo* model of melanoma. Specifically, we delivered tumor-extracted antigens into DCs using BLs and ultrasound, and investigated whether these treated DCs protected mice from lung metastasis.

2. Materials and methods

2.1. Cells

B16/BL6 cells, a C57BL/6-derived melanoma cell line, were cultured in RPMI 1640 (Sigma Co., St. Louis, MO, USA) supplemented with 10% heat inactivated fetal bovine serum (FBS, GIBCO, Invitrogen Co., Carlsbad, CA, USA), 50 U/ml penicillin, and 50 μg/ml streptomycin (Wako Pure Chemical Industries, Osaka, Japan).

2.2. Generation of mouse bone marrow-derived DCs

DCs were generated from bone marrow cells, as described elsewhere [30]. Briefly, bone marrow cells were isolated from C57BL/6 mice and were cultured in RPMI 1640 supplemented with 10% FBS, 50 μM 2-mercaptoethanol (Sigma Co., St. Louis, MO, USA), 50 U/ml penicillin, 50 μg/ml streptomycin, and 40 ng/ml mouse granulocyte-macrophage colony-stimulating factor (GM-CSF, PeproTech Inc., Rocky Hill, NJ, USA). After 8–16 days of culture, non-adherent cells were collected and used as DCs.

2.3. Preparation of BLs

Liposomes composed of 1,2-distearoyl-sn-glycero-phosphatidylcholine (DSPC) (NOF Co., Tokyo, Japan) and 1,2-distearoyl-sn-glycero-3-phosphatidyl-ethanolamine-methoxypolyethyleneglycol (DSPE-PEG (2 k)-OMe (NOF Co.)), 94:6 (mol:mol), were prepared by reverse phase evaporation. BLs were prepared from the liposomes and perfluoropropane (Takachiho Chemical Industrial Co., Ltd., Tokyo, Japan) as reported before [31,32]. Briefly, 5-ml sterilized vials containing 2 ml of the liposome suspension (lipid concentration: 2 mg/ml) were filled with perfluoropropane, capped, and then supercharged with 7.5 ml of perfluoropropane. The vials were placed in a bath-type sonicator (42 kHz, 100 W; BRANSONIC 2510J-DTH, Branson Ultrasonics Co., Danbury, CT, USA) for 5 min to form the BLs. In this method, the liposomes were reconstituted by sonication under the condition of supercharge with perfluoropropane in the 5-ml vial container. At the same time, perfluoropropane would be entrapped within lipids as micelles (composed of DSPC and DSPE-PEG(2k)-OMe), so forming nanobubbles. The lipid nanobubbles were encapsulated within the reconstituted liposomes, the sizes of which were increased from ~150–200 nm to ~500 nm.

2.4. Extraction of antigens from B16/BL6 cells

The extraction of antigens from B16BL/6 cells was performed by a butanol extraction method [33]. B16/BL6 cells were washed twice with phosphate-buffered saline (PBS) and then incubated with PBS containing 2.5% (v/v) 1-butanol. The solution was collected and centrifuged twice at 1600 ×g at 4 °C. The supernatant was dialyzed with water using a Spectra/Por Dialysis Membrane (MWCO: 10,000; Spectrum Laboratories, Inc., Rancho Dominguez, CA, USA). The dialysate then was centrifuged at 1600 ×g at 4 °C, and the resulting supernatant was freeze-dried.

2.5. FITC-dextran or B16/BL6-extracted antigen delivery following inhibition of the endocytic pathway in DCs

B16/BL6-extracted antigens were labeled with Alexa Fluor 633 Succinimidyl Esters (Invitrogen Co., Carlsbad, CA, USA) (Alexa-B16/BL6). DCs were pretreated with OptiMEM (Invitrogen Co.) containing 10 mM NaN_3 for 1 h at 4 °C to inhibit the endocytic pathway [34,35]. After washing the cells, BLs (120 μg) and FITC-dextran (Sigma Co.) or Alexa-B16/BL6 were added to the DCs in OptiMEM containing 10 mM NaN_3. The DCs were exposed to ultrasound (frequency: 2 MHz, duty: 10%, burst rate: 2.0 Hz, intensity 2.0 W/cm^2, time: 3 × 10 s (interval: 10 s)) using a Sonopore 4000 (6-mm diameter probe; Nepa Gene Co. Ltd., Chiba, Japan), then washed with PBS containing 10 mM NaN_3. The delivery efficiency of FITC-dextran or Alexa-B16/BL6 delivery was analyzed by flow cytometry [36].

2.6. Immunization with antigen-loaded DCs following BLs and ultrasound

DCs (2.5×10^5 cells) were pulsed with antigens (50 μg) exposed to ultrasound and/or BLs (120 μg) in a 48-well plate; the contents of 10 wells then were collected, pooled, and seeded into 1 well of a 6-well plate. After 1 h of incubation at 37 °C, the DCs were washed with medium and cultured for 24 h at 37 °C. The cells were washed with PBS, and the DCs (1×10^6 cells/100 μl) then were injected intradermally into the backs of C57BL/6 mice twice with a one-week interval.

2.7. B16/BL6 experimental lung metastasis model

C57BL/6 mice were immunized twice with DCs as described above. Seven days after the second immunization, B16/BL6 cells (1×10^5 cells/100 μl) were injected into the tail vein. The mice were sacrificed two weeks after the tumor cell injection, and the lungs were harvested and fixed in neutral buffered formalin (10%). The number of B16/BL6 colonies present on the surface of each set of lungs was determined by visual inspection using a stereoscopic dissecting microscope [37].

2.8. Statistical analysis

Differences in the number of lung metastatic colonies between the experimental groups were compared using non-repeated measures analysis of variance (ANOVA) with post-hoc Dunnett's test.

3. Results

3.1. FITC-dextran delivery into DCs by BLs and ultrasound

In BL/ultrasound antigen delivery, extracellular antigens are delivered into cells via the formation of transient membrane pores. Therefore, this technique is expected to deliver antigens into DCs as a function of both